IEEE Access
Multidisciplinary | Rapid Review | Open Access Journal

Received March 3, 2019, accepted March 16, 2019, date of publication March 20, 2019, date of current version April 8, 2019.

Digital Object Identifier 10.1109/ACCESS.2019.2906382

Multi-User Cooperative Non-Orthogonal Multiple Access Scheme With Hybrid Full/Half-Duplex User-Assisted Relaying

NINGNING GUO, JIANHUA GE, QIFEI BU, AND CHENSI ZHANG, (Member, IEEE)
State Key Laboratory of Integrated Service Networks, Xidian University, Xi'an 710071, China

Corresponding author: Ningning Guo (nnguo@stu.xidian.edu.cn)

This work was supported by the Collaborative Innovation Center of Information Sensing and Understanding at Xidian University.

ABSTRACT This paper has investigated a downlink non-orthogonal multiple access (NOMA) cooperative scheme with user-assisted relaying, where near users are viewed as decode-and-forward (DF) relays operating full/half-duplex mode to assist multiple far users. Especially, the impact for the randomness of users location on the system performance has also been studied. Further, to overcome the zero diversity gain inherent to full-duplex (FD) operation, the direct link between a base station (BS) and each far user is exploited. The comprehensive performance analysis is conducted through the closed-form expressions in terms of outage probability, the diversity gain, system throughput, and ergodic sum rate. With respect to outage behavior, throughput, and ergodic sum rate, FD-based NOMA outperforms half-duplex (HD) NOMA in the lower signal-to-noise ratio (SNR) region. However, with the negative influence brought by residual loop-interference (LI), the advantage of FD NOMA scheme is not pronounced enough in the high SNR regime. Therefore, according to different SNR levels, we further propose a hybrid relaying scheme that switches opportunistically between the FD and HD modes. Afterward, the mode switching threshold is characterized such that the outage probability of each user is minimized. The simulation results confirm the correctness of our analysis and offer a significant guideline for system design in practice.

INDEX TERMS User relaying, full-duplex, non-orthogonal multiplex access, outage probability, throughput, ergodic sum rate.

I. INTRODUCTION

Spectrum efficiency is of pivotal importance for the next-generation (5G) mobile communication [1], [2]. To this effect, NOMA has caused extremely widespread attention among academia and industry, owing to its ability to accomplish the spectrum multiplexing among multiple users with different power levels [3], [4]. More importantly, since multiple users can be served simultaneously on the same radio resources (i.e., time, frequency and code domain), NOMA offers more massive connectivity and user fairness [4], [5]. With the aid of successive interference cancellation (SIC) at the receiver, multiple-user separation can be handled precisely.

So far, NOMA has been applied extensively to cooperative communication, on the standpoint of extending the coverage of networks [3], [6]–[8]. To be specific, Abbasi *et al.* [6] propose a NOMA-based cooperative relay network with a novel detection strategy and have verified that relay-assisted transmission of amplify-and-forward protocol can obtain full cooperative diversity. Also, the system-level performance investigation of a downlink cooperative NOMA scheme over Nakagami-*m* fading conditions is analyzed in [8], in terms of outage probability and ergodic sum rate. In addition, as reported in [3], the cell-center users not only communicate with the source, but they also are viewed as relay for other cell-edge users. Accordingly, novel cooperative NOMA systems using stochastic geometry are presented in [9] and [10], where the users are distributed randomly around the source node. Leveraging tool from stochastic geometry, the impact of spatial randomness (i.e., BSs, relays or mobile users) on the system reliability can be seen in [9] and [10]. However, as commonly assumed in the above works [3], [5], [6], [8]–[10], HD operation at the

The associate editor coordinating the review of this manuscript and approving it for publication was Yang Tang.

relaying introduces a loss of spectral-efficiency since relay receiving and forwarding requires two time-orthogonal slots.

Compared to HD mode, as a potential tool to enhance system capacity, FD operation allows the data of transmission and reception to accomplish simultaneously over the same radio resource [11]–[13]. While FD relaying is known to suffer from LI, it nonetheless remains feasible as passive or active LI suppression mechanisms develop [14]–[17]. Recently, several researches in [11]–[13] have an insight into the application of FD mode to cooperative NOMA networks, due to the lower latency and lower spectral loss brought by FD operation. Besides, Yue *et al.* [18] and Do *et al.* [19] adopt the full/half-duplex relaying in user-assisted cooperative NOMA scheme. To highlight the potential gain of FD NOMA scheme, a comprehensive study is conducted in [18] through outage probability, ergodic rate and energy efficiency. Additionally, an on/off relaying scheme using either FD or HD mode is introduced in [19], which shows the reduction of performance gap between cell-center and cell-edge users. Further in [20], the near user acting as an FD relaying helps the far user, meanwhile, the optimal power allocation algorithm is exploited to minimize the outage probability.

The aforementioned researches have addressed the application of FD relaying to a cooperative NOMA scheme, however, all these works allow single far user to be better served [12], [13], [18]–[20]. The potential benefits by combining these two pivotal techniques of NOMA and FD mode are still far from being well understood, which is one of the motivations for our paper. In fact, considering the non-uniformity of user distribution in a cell [21], the cell-edge users are required to be better served for guaranteeing user fairness. As discussed in [21] and [22], a novel user pairing scheme in which a cell-center user pairs with multiple cell-edge users has been developed. Compared to conventional pairing scheme, the virtual pairing can ensure every cell-edge user to be paired and further improve spectral efficiency. Meanwhile, Shahab and Shin [23] have considered a time shared NOMA system, where multiple far users communicate with base station through a dedicated FD/HD relaying.

Motivated by [21]–[23], we group a near user and multiple far users in pairs to implement NOMA protocol. Besides, the near user acting as a FD/HD relaying can assist multiple cell-edge users, which further improve the overall reliability of system. Note that every user distributes randomly in a cellular area, the important knowledge of the user locations is worth delving into. Particularly, the distance information between each user and base station enables us to focus on characterizing the statistical properties of channel state information (CSI). Thereby, based on tools from stochastic geometry, the influence of the randomness for users on system performance is also introduced. Furthermore, compared to [20], we observe that the direct link between the BS and each far user is crucial for the performance of FD user relaying scheme.

Based on the above considerations, we investigate a downlink full/half-duplex cooperative NOMA network. Meanwhile, only statistical CSI is available in the transmitter, due to random deployment of users. Compared to the existing literatures, the main contributions of this paper are summarized as follows:

- We aim to coalesce NOMA and FD relaying to improve spectral efficiency of the scheme. Further, in order to better serve multiple cell-edge users, our paper presents a cooperation network consisting of direct link transmission and cooperation phase transmission. Also, we find that, as for far users, the zero diversity gain problem inherent to FD cooperative scheme is overcame by the aid of direct link.
- We focus on the outage performance analysis in terms of FD/HD NOMA systems and take the location of the near and far users into account. Leveraging mathematical tools, exact or approximated expressions of outage probabilities at the near and far users are obtained. Besides, the system throughput can be attained on the basis of the derived outage probability. To obtain more insights, a simple approximation for the outage probability is studied in the high SNR region. Furthermore, we derive the diversity gain of the near and far users to assess the outage behavior.
- To further improve the outage behavior, we aim to investigate a hybrid relaying scheme which can opportunistically operate between FD and HD mode. Additionally, a simple algorithm for determining the level of SNR threshold $\rho_{\mathcal{U}}$ is proposed. Simulation results show that the proposed scheme has the optimal outage behavior in comparison with the pure FD NOMA scheme and the pure HD NOMA system.
- The analysis of ergodic capacity is also necessary. Accordingly, we derive the expressions of analytical and asymptotic ergodic rates in FD/HD NOMA schemes. Also, the slope analysis for ergodic rate is considered in the high SNR region. Regarding to far users, it reveals that the capacity ceilings will limit the ergodic sum rate of the proposed scheme. More notably, the ergodic sum rate of FD NOMA scheme shows better performance improvement in comparison to the HD NOMA one at low and medium SNR region.

In what follows, $\Pr[\cdot]$ denotes probability, $f_Y(\cdot)$ and $F_Y(\cdot)$ symbolize the probability density function (PDF) and the cumulative distribution function (CDF) associated with a random variable (RV) Y, and $\mathbb{E}\{\cdot\}$ represents the expectation operator.

II. SYSTEM MODEL

Consider a DF cooperative NOMA cellular communication network with one base station S and multiple randomly deployed users, as depicted in Fig. 1. To highlight the NOMA protocol, we only investigate two kinds of mobile users: near users (i.e., N_i) and far users (i.e., F_j) [9]. Near users are uniformly located in a circle $\mathcal{D}_N$ with radius R_N, whereas the far users are uniformly deployed in a annulus $\mathcal{D}_F$ with

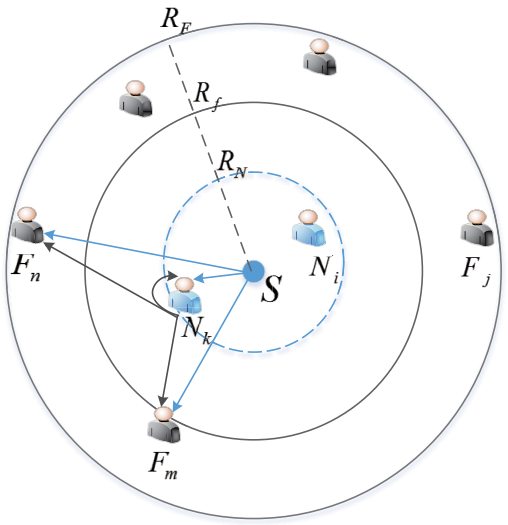

FIGURE 1. System model of downlink NOMA cooperative communication.

inner radius R_f (assuming $R_f \gg R_N$) and outer radius R_F. Importantly, the S is located at the origin of both $\mathcal{D}_N$ and $\mathcal{D}_F$. We assume that the direct link between S and F_j is available, and near users can be generally viewed as dedicated relays to assist the cell-edge users. Being consistent with [12], [18], and [20], we suppose that N_i is equipped with dual antennas with one for transmission and the other for reception, and operates either in FD mode or in HD mode, while the BS and F_j operate in HD operation with a single antenna.[1]

Particularly, we assume that all channels experience additive white Gaussian noise (AWGN) and composite channel fading with both quasi-static Rayleigh fading and large-scale path loss. The complex channel coefficients of $S \to N_i$, $S \to F_j$ and $N_i \to F_j$ are denoted by g_{SN_i}, g_{SF_j} and $g_{N_iF_j}$, respectively. Assuming that the line-of-sight component between the transmit antenna (Tx) and the receive antenna (Rx) at the full-duplex mode is considerably suppressed by antenna isolation, the residual loop/self-interference link at N_i is denoted as g_{LI} and is subjected to Rayleigh fading with the corresponding average power Ω_{LI}, as the same as in [11], [13], [18], and [20].

To highlight the analysis, one near user N_k and the C far users F_l ($l = 1, 2, 3, \cdots, C$) are randomly selected.[2] Further, it is assumed that the distance of N_k from BS is marked as d_{SN_k}, and the C far users' distances away from BS are ranked as $d_{SF_1} \le d_{SF_2} \le \cdots \le d_{SF_C}$. Particularly, we only focus on the performance analysis of the paired user group consisting of the mth far user (i.e., F_m) and the nth far user (i.e., F_n), $m < n$, to carry out the NOMA protocol.[3]

At the time slot j ($j = 1, 2, 3, \ldots$), S broadcasts $x_S[j]$, while N_k, F_m and F_n are ready to receive. $x_S[j]$ is a superposed signal, $x_S[j] = \sqrt{a_k}x_k[j] + \sqrt{a_m}x_m[j] + \sqrt{a_n}x_n[j]$, where the x_i is unity power message intended for the user i, i.e, $\mathbb{E}\{x_i^2\} = 1$, $i \in \{k, m, n\}$ and a_i is the corresponding power allocation factor. Base on the NOMA concept, we assume that $a_n > a_m > a_k$ with $a_k + a_m + a_n = 1$.

Importantly, N_k receives x_S and decodes all users' message successively by means of SIC.[4] Then conditioned on successfully decoding x_m and x_n, N_k will re-superimpose the two decoded message, with different power allocation parameters b and $1-b$, as a signal x_R and forward it to F_m and F_n. Note that $x_R[j] = \sqrt{b}x_n[j - T_d] + \sqrt{1-b}x_m[j - T_d]$, where T_d ($T_d \ge 1$) is the processing delay.

As a result, the observations at N_k, F_i, $i \in \{m, n\}$ can be written respectively by

$$\begin{aligned} y_{N_k}[j] &= g_{SN_k}\sqrt{P_S}x_S[j] + \sqrt{\varpi}\, g_{LI}\sqrt{P_R}t_{LI}[j] + n_{N_k}[j], \\ y_{F_i}[j] &= g_{SF_i}\sqrt{P_S}x_S[j] + g_{N_kF_i}\sqrt{P_R}x_R[j] + n_{F_i}[j]. \end{aligned} \quad (1)$$

where (i) $\varpi \in \{0, 1\}$ is the mode indicator. N_k can work in FD operation if $\varpi = 1$, otherwise N_k works in HD mode; (ii) t_{LI} is loop/self-interference and $t_{LI}[j] = \sqrt{\kappa}x_R[j]$, κ ($0 \le \kappa \le 1$) is the suppressed level of LI after undergoing recent LI cancellation techniques (e.g., passive/active suppression methods) [13], [18], [20]; (iii) P_S and P_R are the transmit powers at S and N_k, respectively; (iv) $n_{N_k}[j] \sim \mathcal{CN}\left(0, \sigma_{N_k}^2\right)$ and $n_{F_i}[j] \sim \mathcal{CN}\left(0, \sigma_{F_i}^2\right)$ are complex additive white Gaussian noise (AWGN).

Suppose that $\sigma_{N_k}^2 = \sigma_{F_i}^2 = \sigma^2$, $i \in \{m, n\}$, we define $\rho_R \triangleq P_R/\sigma^2$ and $\rho \triangleq P_S/\sigma^2$, where ρ and ρ_R denote the transmit SNR at the base station and relaying, respectively [18].

After receiving y_{N_k}, N_k invoking the SIC will firstly decode x_n and remove it, and then N_k decodes x_m and x_k in turn using the same process. So the instantaneous signal-to-noise-plus-interference radio (SINR) at N_k to detect x_n is given by

$$\gamma_{F_n \to N_k} = \frac{a_n\rho\left|g_{SN_k}\right|^2}{\left(1 - a_n\right)\rho\left|g_{SN_k}\right|^2 + \kappa\varpi\,\rho_R|g_{LI}|^2 + 1}. \quad (2)$$

Assuming that x_n is decoded successfully and subtracted completely, the SINR at N_k to detect x_m is given by

$$\gamma_{F_m \to N_k} = \frac{a_m\rho\left|g_{SN_k}\right|^2}{a_k\rho\left|g_{SN_k}\right|^2 + \kappa\varpi\,\rho_R|g_{LI}|^2 + 1}. \quad (3)$$

Lastly, conditioned on x_m being detected successfully, the SINR at N_k to detect its own message is given by

[1] Suppose that the BS and distant users are equipped with multiple antennas, the LI can be eliminated to an extent [18]. However, multiple antenna system needs multiple RF chains, which will add cost in terms of size, power, and hardware. The multi-antenna case will be studied in our future work.

[2] The random selection scheme is leveraged in our paper for two reasons. One reason is that the scheme is a way to bring fairness for each user to access the base station [9], and the second reason is that only statistical CSI is available in our paper.

[3] According to NOMA protocol, our paper mainly concentrate on the typical case of selecting the users with distinct channel gains, as is commonly done in [3] and [8]. Additionally, there may come a case that the selected users possess similar channel gains [21]–[23], which is also an important topic to purse in future works.

[4] Assuming that the perfect SIC is exploited in our paper, our future work will take the decoding error into consideration.

$$\gamma_{N_k} = \frac{a_k \rho \left|g_{SN_k}\right|^2}{\kappa \varpi \rho_R \left|g_{LI}\right|^2 + 1}. \tag{4}$$

The SINRs at F_n to detect its own signal from direct link and relaying link are given respectively by

$$\begin{aligned} \gamma_{S,F_n} &= \frac{a_n \rho \left|g_{SF_n}\right|^2}{\left(1 - a_n\right) \rho \left|g_{SF_n}\right|^2 + 1}, \\ \gamma_{R,F_n} &= \frac{b \rho_R \left|g_{N_k F_n}\right|^2}{\left(1 - b\right) \rho_R \left|g_{N_k F_n}\right|^2 + 1}. \end{aligned} \tag{5}$$

As for F_m, in the direct link transmission, the SINR at F_m to detect the message of F_n and the SINR to detect its own information are written respectively as

$$\begin{aligned} \gamma_{S,F_n \to F_m} &= \frac{a_n \rho \left|g_{SF_m}\right|^2}{\left(1 - a_n\right) \rho \left|g_{SF_m}\right|^2 + 1}, \\ \gamma_{S,F_m} &= \frac{a_m \rho \left|g_{SF_m}\right|^2}{a_k \rho \left|g_{SF_m}\right|^2 + 1}. \end{aligned} \tag{6}$$

For the cooperative transmission, the SINR at F_m to detect firstly x_n and the SINR to detect its own signal, x_m, are expressed respectively as

$$\begin{aligned} \gamma_{R,F_n \to F_m} &= \frac{b \rho_R \left|g_{N_k F_m}\right|^2}{\left(1 - b\right) \rho_R \left|g_{N_k F_m}\right|^2 + 1}, \\ \gamma_{R,F_m} &= \left(1 - b\right) \rho_R \left|g_{N_k F_m}\right|^2. \end{aligned} \tag{7}$$

Assuming the signal from S and the forwarded signal from N_k are resolvable absolutely at the receiving side [12], [18], [24], so that the two signals can be combined by selection combining (SC).[5] Therefore, the instantaneous SINR of F_i, $i \in \{m, n\}$, is given as

$$\gamma_{F_i} = \max\left(\gamma_{S,F_i}, \gamma_{R,F_i}\right). \tag{8}$$

III. DENSITY FUNCTION OF CHANNEL GAINS

In this section, we characterize the distributions of the channel gains, i.e., g_{SN_i}, g_{SF_j} and $g_{N_i F_j}$. Prior to description, we assume that a composite channel fading model is considered [9], i.e., $g_{ij} = \frac{h_{ij}}{\sqrt{1+d_{ij}^{\alpha}}}$, $ij \in \left\{SN_i, SF_j, N_i F_j\right\}$, in which h_{ij} models the small-scale Rayleigh fading with $h_{ij} \sim \mathcal{CN}(0,1)$, d_{ij} denotes the distance between the i and j, as well as α is the path-loss exponent. In general, the path loss exponent takes the value from 2 to 6. Since $\left|h_{ij}\right|^2$ follows exponential distribution, the CDF of $\left|g_{ij}\right|^2$ is given as follows:

$$F_{\left|g_{ij}\right|^2}(x) = \int \left(1 - e^{-(1+r^{\alpha})x}\right) f_{d_{ij}}(r)\, dr, \tag{9}$$

in which d_{ij} depends on the location of the user.

[5] Due to the processing delay T_d, the two signals coming from S and N_k arrive asynchronously at the destinations. Accordingly, SC is more suitable for our scheme where the phase information for each link is unavailable. Compared to maximal radio combining (MRC), SC has lower implementation cost and has no loss in diversity gain [25]. To obtain more insight, our future work will investigate the performance analysis brought by the MRC.

Suppose each near user N_i is uniformly located in $\mathcal{D}_N$, the distribution of the distance between S and any N_i denoted by d_{SN_i} is independent and identically distributed (*i.i.d*) and its PDF can be given by $f_{d_{SN_i}}(r) = \frac{2r}{R_N^2}$. Based on (9) and leveraging the Gaussian-Chebyshev quadrature [9], [26], the CDF of $\left|g_{SN_i}\right|^2$ can be approximated as

$$F_{\left|g_{SN_i}\right|^2}(x) \approx \sum_{p=1}^{P} \frac{\omega_P}{2} \sqrt{1-\phi_p^2} \left(\phi_p + 1\right) \left[1 - e^{-\left(1+T_p^{\alpha}\right)x}\right], \tag{10}$$

where P is the complexity-accuracy tradeoff parameter, $\omega_P = \frac{\pi}{P}$, $T_p = \frac{R_N}{2}\left(\phi_p + 1\right)$ and $\phi_p = \cos\left(\frac{2p-1}{2P}\pi\right)$.

Particularly, when $\alpha = 2$ and after some integral operations, an exact closed-form expression of the equation (9) is given by

$$F_{\left|g_{SN_i}\right|^2}(x)\Big|_{\alpha=2} = 1 - \frac{e^{-x}}{R_N^2 x} + \frac{e^{-\left(1+R_N^2\right)x}}{R_N^2 x}. \tag{11}$$

Importantly, we focus on the analysis of C selected randomly distant users. Note that each far user F_l is uniformly distributed in $\mathcal{D}_F$, the PDF of the unordered distance variable from S to F_l is $f_{d_{SF_l}}(r) = \frac{2r}{R_F^2 - R_f^2}$. In this case, the PDF of the ordered distance variable $\tilde{d}_{SF_l}$, $l = 1, 2, \cdots, C$, can be expressed leveraging the theory of order statistics as [27]

$$\begin{aligned} f_{\tilde{d}_{SF_l}}(r) = \frac{C!}{(C-l)!\,(l-1)!} f_{d_{SF_l}}(r) \left[F_{d_{SF_l}}(r)\right]^{l-1} \\ \times \left[1 - F_{d_{SF_l}}(r)\right]^{C-l}, \end{aligned} \tag{12}$$

where $F_{d_{SF_l}}(r) = \frac{r^2 - R_f^2}{R_F^2 - R_f^2}$ is the corresponding CDF of d_{SF_l}.

As such, substituting (12) into (9), a Gaussian-Chebyshev approximation of $F_{\left|g_{SF_l}\right|^2}(x)$ can be derived as follows:

$$\begin{aligned} &F_{\left|g_{SF_l}\right|^2}(x) \\ &\approx C_l \sum_{q=1}^{Q} \omega_Q \sqrt{1-\phi_q^2} \left(R_F - R_f\right) \left[1 - e^{-\left(1+T_q^{\alpha}\right)x}\right] \\ &\quad \times \frac{T_q \left(T_q^2 - R_f^2\right)^{l-1} \left(R_F^2 - T_q^2\right)^{C-l}}{\left(R_F^2 - R_f^2\right)^{C}}, \end{aligned} \tag{13}$$

where $C_l = \frac{C!}{(C-l)!(l-1)!}$, Q is the factor to ensure a complexity-accuracy tradeoff, $\omega_Q = \pi/Q$, $\phi_q = \cos\left(\frac{2q-1}{2Q}\pi\right)$ and $T_q = \frac{R_F - R_f}{2}\phi_q + \frac{R_F + R_f}{2}$.

Corollary 1: Note that if $\alpha = 2$, an exact expression of $F_{\left|g_{SF_l}\right|^2}(x)$ is derived by

$$\begin{aligned} &F_{\left|g_{SF_l}\right|^2}(x)\Big|_{\alpha=2} \\ &= C_l \sum_{p1=0}^{C-l} \binom{C-l}{p1} (-1)^{p1} \left[\frac{1}{l+p1}\right. \end{aligned}$$

$$- \frac{e^{-\left(1+R_f^2\right)x} x^{-(l+p1)} \gamma\left(l+p1, \left(R_F^2-R_f^2\right)x\right)}{\left(R_F^2-R_f^2\right)^{l+p1}}\Bigg], \quad (14)$$

where $\gamma(\nu,\mu) = \int_0^{\mu} x^{\nu-1}e^{-x}dx$ *is the incomplete Gamma function [28, Eq.(3.351.1)].*

Proof : See Appendix A. ■

Importantly, the distance between N_i and F_l can be calculated as: $d_{N_iF_l} = \sqrt{d_{SN_i}^2 + d_{SF_l}^2 - 2d_{SN_i}d_{SF_l}\cos(\angle N_iSF_l)}$. Assuming $d_{SF_l} \gg d_{SN_i}$, therefore an approximation value of $d_{N_iF_l}$, namely, $d_{N_iF_l} \approx d_{SF_l}$, has been made in the following for the convenience of theoretical derivation analysis. Along the lines of the derivation of (12) and (13), we generally assume that $|g_{N_iF_l}|^2$ and $|g_{SF_l}|^2$ are *i.i.d* variables.

IV. OUTAGE PROBABILITY ANALYSIS

As a benchmark evaluation of system performance, the outage behavior for users N_k, F_n and F_m is characterized in what follows. Particularly, since base station transmits signals at constant rates in the delay-limited transmission mode, the outage probability is used for estimating whether the predefined data rates are appropriate. Correspondingly, an outage event will happen if the SINR falls below the target threshold [8].

A. ANALYTICAL ANALYSIS

1) OUTAGE PROBABILITY OF N_K

Based on the NOMA principle, the complementary event of outage at N_k is defined as: N_k can successfully decode x_n, x_m and its own signal x_k.

As a result, the outage probability for N_k is described as

$$\mathcal{P}_{N_k}^{FD} = 1 - \Pr\left(\gamma_{F_n\to N_k} > \gamma_{th_n}^{FD}, \gamma_{F_m\to N_k} > \gamma_{th_m}^{FD}, \gamma_{N_k} > \gamma_{th_k}^{FD}\right), \quad (15)$$

where $\gamma_{th_i}^{FD} = 2^{\mathcal{R}_i} - 1$ and $\mathcal{R}_i$ is the target rate at N_k to detect x_i, $i \in \{k, m, n\}$. Next, the outage probability of the near user N_k is shown in the Theorem 1.

Theorem 1: The outage probability of the nearby user N_k *can be approximated as*

$$\mathcal{P}_{N_k}^{FD} \approx \sum_{p=1}^{P} \frac{\omega_P}{2}\sqrt{1-\phi_p^2}\left(\phi_p+1\right) \times \left[1 - \frac{\rho e^{-\frac{\theta_1\left(1+T_p^{\alpha}\right)}{\rho}}}{\rho + \rho_R\kappa\varpi\Omega_{LI}\theta_1\left(1+T_p^{\alpha}\right)}\right], \quad (16)$$

in which $\varsigma_1 = \frac{\gamma_{th_n}^{FD}}{a_n-(1-a_n)\gamma_{th_n}^{FD}}$, $\beta_1 = \frac{\gamma_{th_m}^{FD}}{a_m-a_k\gamma_{th_m}^{FD}}$, $\chi_1 = \frac{\gamma_{th_k}^{FD}}{a_k}$, *and we have a definition:* $\theta_1 \triangleq \max(\varsigma_1, \beta_1, \chi_1)$. *It is worthy of note that approximation (16) is obtained on the conditions of* $\gamma_{th_n}^{FD} < \frac{a_n}{1-a_n}$ *and* $\gamma_{th_m}^{FD} < \frac{a_m}{a_k}$.

Proof: Using (2), (3) and (4), the equation (15) can be rewritten as

$$\begin{aligned}\mathcal{P}_{N_k}^{FD} &= 1 - \Pr\left[|g_{SN_k}|^2 > \frac{\max(\varsigma_1,\beta_1,\chi_1)}{\rho}\left(\kappa\varpi\rho_R|g_{LI}|^2+1\right)\right] \\ &= \int_0^{\infty} F_{|g_{SN_k}|^2}\left[\frac{\theta_1}{\rho}\left(\kappa\varpi\rho_R x+1\right)\right] f_{|g_{LI}|^2}(x)\,dx. \quad (17)\end{aligned}$$

Next, by substituting (10) into (17) and taking some integral manipulations, the approximated outage probability of N_k can be obtained in (16). The proof is complete. ■

Corollary 2: For $\alpha = 2$, *an exact closed-form expression of the outage probability for* N_k *is expressed as*

$$\begin{aligned}\mathcal{P}_{N_k}^{FD}\Big|_{\alpha=2} &= 1 + \frac{\rho e^{\frac{1}{\kappa\rho_R\varpi\Omega_{LI}}}}{\kappa\rho_R\varpi R_N^2\Omega_{LI}\theta_1}\left\{Ei\left[-\left(\frac{1}{\kappa\rho_R\varpi\Omega_{LI}}+\frac{\theta_1}{\rho}\right)\right]\right. \\ &\quad \left. - Ei\left[-\left(\frac{1}{\kappa\rho_R\varpi\Omega_{LI}}+\frac{\theta_1\left(1+R_N^2\right)}{\rho}\right)\right]\right\}, \quad (18)\end{aligned}$$

where $Ei(\cdot)$ *denotes the exponential integral function.*

Proof: Similar to the derivations in (17), substituting (14) into (17), we can obtain (19), as shown at the top of the next page, where the step $\langle 1\rangle$ is obtained by using $t = (\kappa\varpi\rho_R x+1)/\rho$ and some manipulations.

According to [28, Eq.(3.352.2)], φ from (19) can be derived as

$$\begin{aligned}\varphi = &-Ei\left[-\left(\frac{1}{\kappa\rho_R\varpi\Omega_{LI}}+\frac{\theta_1}{\rho}\right)\right] \\ &+ Ei\left\{-\left[\frac{1}{\kappa\rho_R\varpi\Omega_{LI}}+\frac{\theta_1\left(1+R_N^2\right)}{\rho}\right]\right\}. \quad (20)\end{aligned}$$

Finally, by substituting (20) into (19), (18) can be attained. The proof is done. ■

Particularly, similar to the derivations in (16), the outage probability of N_k for HD NOMA can be given in the following corollary.

Corollary 3: Let $\varpi = 0$, *the outage probability of* N_k *for HD NOMA is expressed by*

$$\mathcal{P}_{N_k}^{HD} \approx \frac{1}{2}\sum_{p=1}^{P}\omega_P\sqrt{1-\phi_p^2}\left(\phi_p+1\right)\left[1-e^{\frac{\theta_1^*\left(1+T_p^{\alpha}\right)}{\rho}}\right], \quad (21)$$

and for $\alpha = 2$, *we have*

$$\mathcal{P}_{N_k}^{HD}\Big|_{\alpha=2} = 1 - \frac{\rho e^{-\frac{\theta_1^*}{\rho}}}{R_N^2\theta_1^*} + \frac{\rho e^{-\frac{\theta_1^*\left(1+R_N^2\right)}{\rho}}}{R_N^2\theta_1^*}, \quad (22)$$

where $\gamma_{th_i}^{HD} = 2^{2\mathcal{R}_i} - 1$, $i \in \{k, m, n\}$, *as well as* $\varsigma_1^* = \frac{\gamma_{th_n}^{HD}}{a_n-(1-a_n)\gamma_{th_n}^{HD}}$ *with* $\gamma_{th_n}^{HD} < \frac{a_n}{1-a_n}$, $\beta_1^* = \frac{\gamma_{th_m}^{HD}}{a_m-a_k\gamma_{th_m}^{HD}}$ *with* $\gamma_{th_m}^{HD} < \frac{a_m}{a_k}$, $\chi_1^* = \frac{\gamma_{th_k}^{HD}}{a_k}$ *and* $\theta_1^* \triangleq \max\left(\varsigma_1^*, \beta_1^*, \chi_1^*\right)$.

In the following, it is worthy of note that the cooperative phase transmission depends on the event A_i,

$$\mathcal{P}_{N_k}^{FD}\Big|_{\alpha=2} = \frac{1}{\Omega_{LI}}\int_0^{\infty}\left[1-\frac{\rho e^{-\frac{\theta_1}{\rho}(\kappa\varpi\rho_R x+1)}}{R_N^2\theta_1(\kappa\varpi\rho_R x+1)}+\frac{\rho e^{-\frac{\theta_1}{\rho}\left(1+R_N^2\right)(\kappa\varpi\rho_R x+1)}}{R_N^2\theta_1(\kappa\varpi\rho_R x+1)}\right]e^{-\frac{x}{\Omega_{LI}}}dx$$
$$\underset{\langle 1\rangle}{=} 1-\frac{\rho e^{\frac{1}{\kappa\varpi\rho_R\Omega_{LI}}}}{\kappa\varpi\rho_R R_N^2\Omega_{LI}\theta_1}\underbrace{\left\{\int_{\frac{1}{\rho}}^{\infty}\frac{e^{-\left(\frac{\rho}{\kappa\varpi\rho_R\Omega_{LI}}+\theta_1\right)t}}{t}dt-\int_{\frac{1}{\rho}}^{\infty}\frac{e^{-\left[\frac{\rho}{\kappa\varpi\rho_R\Omega_{LI}}+\theta_1\left(1+R_N^2\right)\right]t}}{t}dt\right\}}_{\varphi} \tag{19}$$

$$\mathcal{P}_{F_n}^{FD}\Big|_{\alpha=2} = C_n\sum_{p1=0}^{C-n}\binom{C-n}{p1}(-1)^{p1}\left[\frac{1}{n+p1}-\frac{e^{-\frac{\psi_f\varsigma_1}{\rho}}\rho^{(n+p1)}\gamma\left(n+p1,\frac{\psi_F\varsigma_1}{\rho}\right)}{(\psi_F\varsigma_1)^{n+p1}}\right]\left\{1+\frac{n_0\rho e^{\frac{n_0}{\rho_R}}}{\theta_2\rho_R R_N^2}\left\{Ei\left[-\left(\frac{n_0}{\rho_R}+\frac{\theta_2}{\rho}\right)\right]\right.\right.$$
$$\left.\left.-\ Ei\left[-\left(\frac{n_0}{\rho_R}+\frac{\theta_2\psi_N}{\rho}\right)\right]\right\}\right\}+\frac{{C_n}^2 n_0\rho e^{\frac{n_0}{\rho_R}}}{\theta_2\rho_R R_N^2}\sum_{p1=0}^{C-n}\sum_{p2=0}^{C-n}\binom{C-n}{p1}\binom{C-n}{p2}$$
$$\times\left\{-Ei\left[-\left(\frac{n_0}{\rho_R}+\frac{\theta_2}{\rho}\right)\right]+Ei\left[-\left(\frac{n_0}{\rho_R}+\frac{\theta_2\psi_N}{\rho}\right)\right]\right\}$$
$$\times(-1)^{p1+p2}\left[\frac{1}{n+p1}-\frac{e^{-\frac{\psi_f\varsigma_1}{\rho}}\rho^{(n+p1)}\gamma\left(n+p1,\frac{\psi_F\varsigma_1}{\rho}\right)}{(\psi_F\varsigma_1)^{n+p1}}\right]\left[\frac{1}{n+p2}-\frac{e^{-\frac{\psi_f\tau_1}{\rho_R}}\rho_R{}^{(n+p2)}\gamma\left(n+p2,\frac{\psi_F\tau_1}{\rho_R}\right)}{(\psi_F\tau_1)^{n+p2}}\right], \tag{26}$$

$$\mathcal{P}_{F_n}^{HD}\Big|_{\alpha=2} = C_n\sum_{p1=0}^{C-n}\binom{C-n}{p1}(-1)^{p1}\left[\frac{1}{n+p1}-\frac{e^{-\frac{\psi_f\varsigma_1^*}{\rho}}\rho^{(n+p1)}\gamma\left(n+p1,\frac{\psi_F\varsigma_1^*}{\rho}\right)}{\left(\psi_F\varsigma_1^*\right)^{n+p1}}\right]\left[1-\frac{\rho\left(e^{-\frac{\theta_2^*}{\rho}}-e^{-\frac{\psi_N\theta_2^*}{\rho}}\right)}{R_N^2\theta_2^*}\right]$$
$$+C_n^2\sum_{p1=0}^{C-n}\sum_{p2=0}^{C-n}\binom{C-n}{p1}\binom{C-n}{p2}(-1)^{p1+p2}\left[\frac{1}{n+p1}-\frac{e^{-\frac{\psi_f\varsigma_1^*}{\rho}}\rho^{(n+p1)}\gamma\left(n+p1,\frac{\psi_F\varsigma_1^*}{\rho}\right)}{\left(\psi_F\varsigma_1^*\right)^{n+p1}}\right]$$
$$\times\left[\frac{1}{n+p2}-\frac{e^{-\frac{\psi_f\tau_1^*}{\rho_R}}\rho_R{}^{(n+p2)}\gamma\left(n+p2,\frac{\psi_F\tau_1^*}{\rho_R}\right)}{\left(\psi_F\tau_1^*\right)^{n+p2}}\right]\left[\frac{\rho\left(e^{-\frac{\theta_2^*}{\rho}}-e^{-\frac{\psi_N\theta_2^*}{\rho}}\right)}{R_N^2\theta_2^*}\right], \tag{29}$$

which is defined as the signals x_m and x_n can be detected successfully at N_k. Accordingly, we have $\mathcal{P}_{A_i} = \Pr\left(\gamma_{F_n\to N_k} > \gamma_{th_n}^{FD}, \gamma_{F_m\to N_k} > \gamma_{th_m}^{FD}\right)$.

Further, according to eqs (2) and (3), $\mathcal{P}_{A_i}$ can be approximated as

$$\mathcal{P}_{A_i} \approx 1-\frac{\omega_P}{2}\sum_{p=1}^{P}\sqrt{1-\phi_p^2}\left(\phi_p+1\right)\times\left[1-\frac{\rho e^{-\frac{\theta_2\left(1+T_p^{\alpha}\right)}{\rho}}}{\rho+\kappa\varpi\rho_R\Omega_{LI}\theta_2\left(1+T_p^{\alpha}\right)}\right], \tag{23}$$

where $\theta_2 \triangleq \max(\varsigma_1, \beta_1)$.

2) OUTAGE PROBABILITY OF F_N

The outage event occurs as follows: (i) F_n cannot detect its own information x_n from x_S when the event A_i fails; (ii) The received SINR after SC at F_n is below its target threshold when the event A_i happens. Therefore, the outage probability of F_n can be described as

$$\mathcal{P}_{F_n}^{FD} = \left(1-\mathcal{P}_{A_i}\right)\Pr\left(\gamma_{S,F_n} < \gamma_{th_n}^{FD}\right)+\mathcal{P}_{A_i}\Pr\left(\gamma_{F_n} < \gamma_{th_n}^{FD}\right). \tag{24}$$

The expression of outage probability for F_n is presented in the following theorem.

Theorem 2: Assuming $d_{N_k F_n} \approx d_{SF_n}$, the outage probability of F_n can be approximated as follows:

$$\begin{aligned}
&\mathcal{P}_{F_n}^{FD} \\
&\approx \eta_n \sum_{p=1}^{P}\sum_{q=1}^{Q} \xi_q^n \zeta_p \left[1 - e^{-\frac{\left(1+T_q^\alpha\right)\varsigma_1}{\rho}}\right] \\
&\quad \times \left[1 - \frac{\rho e^{-\frac{\theta_2\left(1+T_p^\alpha\right)}{\rho}}}{\rho + \kappa\varpi\rho_R\Omega_{LI}\theta_2\left(1+T_p^\alpha\right)}\right] \\
&\quad + \eta_n^2 \sum_{q=1}^{Q}\sum_{q1=1}^{Q} \xi_q^n \xi_{q1}^n \left[1 - e^{-\frac{\left(1+T_q^\alpha\right)\varsigma_1}{\rho}}\right]\left[1 - e^{-\frac{\left(1+T_{q1}^\alpha\right)\tau_1}{\rho_R}}\right] \\
&\quad \times \left\{1 - \sum_{p=1}^{P}\zeta_p\left[1 - \frac{\rho e^{-\frac{\theta_2\left(1+T_p^\alpha\right)}{\rho}}}{\rho + \kappa\varpi\rho_R\Omega_{LI}\theta_2\left(1+T_p^\alpha\right)}\right]\right\}, \quad (25)
\end{aligned}$$

where $\varpi = 1$, $\tau_1 = \frac{\gamma_{th_n}^{FD}}{b-(1-b)\gamma_{th_n}^{FD}}$ *with*

$$\begin{aligned}
&\gamma_{th_n}^{FD} < \frac{b}{1-b}, \quad \eta_n = \frac{C_n\omega_Q\left(R_F - R_f\right)}{\left(R_F^2 - R_f^2\right)^C}, \\
&C_n = \frac{C!}{(C-n)!\,(n-1)!}, \quad \xi_q^n = T_q\sqrt{\left(1-\phi_q^2\right)} \\
&\quad \times \left(T_q^2 - R_f^2\right)^{n-1}\left(R_F^2 - T_q^2\right)^{C-n}, \quad \xi_{q1}^n \\
&\quad = T_{q1}\sqrt{\left(1-\phi_{q1}^2\right)}\left(T_{q1}^2 - R_f^2\right)^{n-1}\left(R_F^2 - T_{q1}^2\right)^{C-n}, \\
&\quad \textit{and } \zeta_p = \frac{\omega_P}{2}\left(\phi_p + 1\right)\sqrt{\left(1-\phi_p^2\right)}.
\end{aligned}$$

Proof: See Appendix B. ■

Corollary 4: For the special case $\alpha = 2$, the outage probability of F_n can be calculated exactly as (26), shown at the top of the previous page, in which $n_0 = \frac{1}{\kappa\varpi\Omega_{LI}}$, $\psi_N = 1 + R_N^2$, $\psi_f = 1 + R_f^2$ and $\psi_F = R_F^2 - R_f^2$.

Proof: Similar to the derivations in (23), the exact expression of $\mathcal{P}_{A_i}$ for $\alpha = 2$ is given by

$$\begin{aligned}
&\mathcal{P}_{A_i}\big|_{\alpha=2} \\
&= \frac{\rho e^{\frac{1}{\kappa\rho_R\varpi\Omega_{LI}}}}{\kappa\varpi\rho_R R_N^2\Omega_{LI}\theta_2}\left\{-Ei\left[-\left(\frac{1}{\kappa\rho_R\varpi\Omega_{LI}} + \frac{\theta_2}{\rho}\right)\right]\right. \\
&\quad \left. + Ei\left[-\left(\frac{1}{\kappa\rho_R\varpi\Omega_{LI}} + \frac{\theta_2\left(1+R_N^2\right)}{\rho}\right)\right]\right\}. \quad (27)
\end{aligned}$$

Further, using the similar derivations in Appendix B, utilizing the CDFs of $F_{|g_{SF_n}|^2}(x)\Big|_{\alpha=2}$ and $F_{|g_{N_k F_n}|^2}(x)\Big|_{\alpha=2}$, as well as combining (27), the exact expression for the outage probability of F_n is obtained and the proof is done. ■

Corollary 5: Similarly, the outage probability of F_n for HD NOMA, namely $\varpi = 0$, is given by

$$\begin{aligned}
&\mathcal{P}_{F_n}^{HD} \\
&\approx \eta_n \sum_{q=1}^{Q}\sum_{p=1}^{P} \zeta_p \xi_q^n \left[1 - e^{-\frac{\theta_2^*\left(1+T_p^\alpha\right)}{\rho}}\right]\left[1 - e^{-\frac{\left(1+T_q^\alpha\right)\varsigma_1^*}{\rho}}\right] \\
&\quad + \eta_n^2 \sum_{q=1}^{Q}\sum_{q1=1}^{Q} \xi_q^n \xi_{q1}^n \left[1 - e^{-\frac{\left(1+T_q^\alpha\right)\varsigma_1^*}{\rho}}\right] \\
&\quad \times \left[1 - e^{-\frac{\left(1+T_{q1}^\alpha\right)\tau_1^*}{\rho_R}}\right]\left\{1 - \sum_{p=1}^{P}\zeta_p\left[1 - e^{-\frac{\theta_2^*\left(1+T_p^\alpha\right)}{\rho}}\right]\right\}, \quad (28)
\end{aligned}$$

Besides, the outage probability of F_n for HD NOMA scheme with the special case $\alpha = 2$ can be obtained in (29), as shown at the top of the previous page, in which $\theta_2^* \triangleq \max\left(\varsigma_1^*, \beta_1^*\right)$ and $\tau_1^* = \frac{\gamma_{th_n}^{HD}}{b-(1-b)\gamma_{th_n}^{HD}}$ with $\gamma_{th_n}^{HD} < \frac{b}{1-b}$.

3) OUTAGE PROBABILITY OF F_M

The outage events of F_m are described as follows: (i) After receiving x_S, x_m cannot be detected at F_m when the event A_i fails; (ii) F_m cannot detect its own message after receiving the signals from direct link and relaying link, although the event A_i happens. As a result, the outage probability of F_m is expressed as

$$\begin{aligned}
&\mathcal{P}_{F_m}^{FD} \\
&= \left(1 - \mathcal{P}_{A_i}\right)\underbrace{\left[1 - \Pr\left(\gamma_{S,F_n\to F_m} > \gamma_{th_n}^{FD}, \gamma_{S,F_m} > \gamma_{th_m}^{FD}\right)\right]}_{J_1} \\
&\quad + \mathcal{P}_{A_i}\left[1 - \Pr\left(\gamma_{S,F_n\to F_m} > \gamma_{th_n}^{FD}, \gamma_{S,F_m} > \gamma_{th_m}^{FD}\right)\right] \\
&\quad \times \underbrace{\left[1 - \Pr\left(\gamma_{R,F_n\to F_m} > \gamma_{th_n}^{FD}, \gamma_{R,F_m} > \gamma_{th_m}^{FD}\right)\right]}_{J_2}. \quad (30)
\end{aligned}$$

To further obtain an intuitional result, the outage probability of F_m is presented in the next theorem.

Theorem 3: Suppose $d_{N_k F_m} \approx d_{SF_m}$, the approximation of the outage probability for F_m is expressed by

$$\begin{aligned}
&\mathcal{P}_{F_m}^{FD} \\
&\approx \eta_m \sum_{p=1}^{P}\sum_{q2=1}^{Q} \zeta_p \xi_{q2}^m \left[1 - e^{-\frac{\left(1+T_{q2}^\alpha\right)\theta_2}{\rho}}\right] \\
&\quad \times \left[1 - \frac{\rho e^{-\frac{\theta_2\left(1+T_p^\alpha\right)}{\rho}}}{\rho + \kappa\varpi\rho_R\Omega_{LI}\theta_2\left(1+T_p^\alpha\right)}\right] \\
&\quad + \eta_m^2 \sum_{q2=1}^{Q}\sum_{q3=1}^{Q} \xi_{q2}^m \xi_{q3}^m \left[1 - e^{-\frac{\left(1+T_{q2}^\alpha\right)\theta_2}{\rho}}\right]\left[1 - e^{-\frac{\left(1+T_{q3}^\alpha\right)\theta_3}{\rho_R}}\right] \\
&\quad \times \left\{1 - \sum_{p=1}^{P}\zeta_p\left[1 - \frac{\rho e^{-\frac{\theta_2\left(1+T_p^\alpha\right)}{\rho}}}{\rho + \kappa\varpi\rho_R\Omega_{LI}\theta_2\left(1+T_p^\alpha\right)}\right]\right\},
\end{aligned}$$

$$\mathcal{P}_{F_m}^{FD}\Big|_{\alpha=2} = C_m \sum_{p3=0}^{C-m} \binom{C-m}{p3} (-1)^{p3} \left[\frac{1}{m+p3} - \frac{e^{-\frac{\psi_f \theta_2}{\rho}} \rho^{(m+p3)} \gamma\left(m+p3, \frac{\psi_F \theta_2}{\rho}\right)}{(\psi_F \theta_2)^{m+p3}} \right] \left\{ 1 + \frac{n_0 \rho e^{\frac{n_0}{\rho_R}}}{\theta_2 \rho_R R_N^2} \left\{ Ei\left[-\left(\frac{n_0}{\rho_R} + \frac{\theta_2}{\rho} \right) \right] \right.\right.$$
$$\left.\left. - Ei\left[-\left(\frac{n_0}{\rho_R} + \frac{\theta_2 \psi_N}{\rho} \right) \right] \right\} \right\} + \frac{C_m{}^2 n_0 \rho e^{\frac{n_0}{\rho_R}}}{\theta_2 \rho_R R_N^2} \sum_{p3=0}^{C-m} \sum_{p4=0}^{C-m} \binom{C-m}{p3} \binom{C-m}{p4}$$
$$\times \left\{ -Ei\left[-\left(\frac{n_0}{\rho_R} + \frac{\theta_2}{\rho} \right) \right] + Ei\left[-\left(\frac{n_0}{\rho_R} + \frac{\theta_2 \psi_N}{\rho} \right) \right] \right\}$$
$$\times (-1)^{p3+p4} \left[\frac{1}{m+p3} - \frac{e^{-\frac{\psi_f \theta_2}{\rho}} \rho^{(m+p3)} \gamma\left(m+p3, \frac{\psi_F \theta_2}{\rho}\right)}{(\psi_F \theta_2)^{m+p3}} \right] \left[\frac{1}{m+p4} - \frac{e^{-\frac{\psi_f \theta_3}{\rho_R}} \rho_R{}^{(m+p4)} \gamma\left(m+p4, \frac{\psi_F \theta_3}{\rho_R}\right)}{(\psi_F \theta_3)^{m+p4}} \right]. \tag{32}$$

$$\mathcal{P}_{F_m}^{HD}\Big|_{\alpha=2} = C_m \sum_{p3=0}^{C-m} \binom{C-m}{p3} (-1)^{p3} \left[\frac{1}{m+p3} - \frac{e^{-\frac{\psi_f \theta_2^*}{\rho}} \rho^{(m+p3)} \gamma\left(m+p3, \frac{\psi_F \theta_2^*}{\rho}\right)}{\left(\psi_F \theta_2^*\right)^{m+p3}} \right] \left[1 - \frac{\rho\left(e^{-\frac{\theta_2^*}{\rho}} - e^{-\frac{\psi_N \theta_2^*}{\rho}} \right)}{R_N^2 \theta_2^*} \right]$$
$$+ C_m^2 \sum_{p3=0}^{C-m} \sum_{p4=0}^{C-m} \binom{C-m}{p3} \binom{C-m}{p4} (-1)^{p3+p4} \left[\frac{1}{m+p3} - \frac{e^{-\frac{\psi_f \theta_2^*}{\rho}} \rho^{(m+p3)} \gamma\left(m+p3, \frac{\psi_F \theta_2^*}{\rho}\right)}{\left(\psi_F \theta_2^*\right)^{m+p3}} \right]$$
$$\times \left[\frac{1}{m+p4} - \frac{e^{-\frac{\psi_f \theta_3^*}{\rho_R}} \rho_R{}^{(m+p4)} \gamma\left(m+p4, \frac{\psi_F \theta_3^*}{\rho_R}\right)}{\left(\psi_F \theta_3^*\right)^{m+p4}} \right] \left[\frac{\rho\left(e^{-\frac{\theta_2^*}{\rho}} - e^{-\frac{\psi_N \theta_2^*}{\rho}} \right)}{R_N^2 \theta_2^*} \right]. \tag{34}$$

(31)

in which $\eta_m = \frac{C_m \omega_Q (R_F - R_f)}{\left(R_F^2 - R_f^2\right)^C}$, *and* $C_m = \frac{C!}{(C-m)!(m-1)!}$, $\xi_{q2}^m = T_{q2}\sqrt{1-\phi_{q2}^2}\left(T_{q2}^2 - R_f^2\right)^{m-1}\left(R_F^2 - T_{q2}^2\right)^{C-m}$ *and* $\xi_{q3}^m = T_{q3}\sqrt{1-\phi_{q3}^2}\left(T_{q3}^2 - R_f^2\right)^{m-1}\left(R_F^2 - T_{q3}^2\right)^{C-m}$.

Proof: See Appendix C. ■

Corollary 6: If $\alpha = 2$, *an exact expression for the outage probability of* F_m *is presented as (32), shown at the top of this page.*

Proof: Along the lines of the similar derivations in Appendix C and using the formulas (14) and (27), the equation (32) can be easily obtained. The proof is complete. ■

Corollary 7: In the same way, the outage probability of F_m *for HD NOMA, i.e.,* $\varpi = 0$, *is given by*

$$\mathcal{P}_{F_m}^{HD} \approx \eta_m \sum_{q2=1}^{Q} \sum_{p=1}^{P} \zeta_p \xi_{q2}^m \left[1 - e^{-\frac{\theta_2^*\left(1+T_p^\alpha\right)}{\rho}} \right] \left[1 - e^{-\frac{\left(1+T_{q2}^\alpha\right)\theta_2^*}{\rho}} \right]$$
$$+ \eta_m^2 \sum_{q2=1}^{Q} \sum_{q3=1}^{Q} \xi_{q2}^m \xi_{q3}^m \left[1 - e^{-\frac{\left(1+T_{q2}^\alpha\right)\theta_2^*}{\rho}} \right]$$
$$\times \left[1 - e^{-\frac{\left(1+T_{q3}^\alpha\right)\theta_3^*}{\rho_R}} \right] \left\{ 1 - \sum_{p=1}^{P} \zeta_p \left[1 - e^{-\frac{\theta_2^*\left(1+T_p^\alpha\right)}{\rho}} \right] \right\}, \tag{33}$$

where $\theta_3^* \triangleq \max\left(\tau_1^*, \xi_1^*\right)$ *and* $\xi_1^* = \frac{\gamma_{th_m}^{HD}}{1-b}$.

Specially, if $\alpha = 2$ *and* $\varpi = 0$, *the outage probability of* F_m *for HD NOMA can be calculated accurately in (34), shown at the top of this page.*

B. ASYMPTOTIC ANALYSIS

To assess the variation trend of the outage probability in high SNR region, the asymptotic diversity analysis is discussed. A definition of the diversity order is expressed as follows:

$$d = -\lim_{\rho \to \infty} \frac{\log \mathcal{P}(\rho)}{\log \rho}. \tag{35}$$

1) THE NEAR USER N_K

In the high SNR regime, i.e., $\rho \to \infty$, we assume $\rho_R = \lambda\rho$ and λ goes from zero to one [13]. Using the fact that $e^x \underset{x \to 0}{\sim} 1$ when $x \to 0$, therefore equation (16) can be further

approximated as

$$\mathcal{P}_{N_k}^{FD,\infty} \approx \sum_{p=1}^{P} \frac{\omega_P}{2} \sqrt{1-\phi_p^2}\left(\phi_p+1\right) \times \left[1-\frac{1}{1+\kappa\varpi\lambda\Omega_{LI}\theta_1\left(1+T_p^{\alpha}\right)}\right]. \quad (36)$$

For $\varpi = 0$ and using $1-e^{-x} \underset{x\to 0}{\sim} x$, a high SNR approximation of (21) is expressed by

$$\mathcal{P}_{N_k}^{HD,\infty} \approx \frac{1}{2}\sum_{p=1}^{P} \omega_P \sqrt{1-\phi_p^2}\left(\phi_p+1\right)\frac{\left(1+T_p^{\alpha}\right)\theta_1^*}{\rho}. \quad (37)$$

Remark 1: Substituting (36) and (37) into (35), we can easily learn that $d_{N_k}^{FD} = 0$ and $d_{N_k}^{HD} = 1$, respectively. Intuitively, when $\rho \to \infty$, the value of $\mathcal{P}_{N_k}^{FD,\infty}$ is a constant which is not associated with ρ. Accordingly, as for near user N_k, there is an error floor in FD NOMA scheme, while the outage probability in HD NOMA could keep decreasing when $\rho \to \infty$. This could be due to the effect of residual LI, which is the nature of the FD relaying [18], [29].

2) THE FAR USER F_N

Based on the analytical expressions in (25) and (28), the asymptotic outage probability of F_n for FD/HD cooperative NOMA can be expressed respectively as follows:

$$\mathcal{P}_{F_n}^{FD,\infty} \approx \eta_n \sum_{p=1}^{P}\sum_{q=1}^{Q}\zeta_p\xi_q^n\frac{\left(1+T_q^{\alpha}\right)\varsigma_1}{\rho} \times \left[1-\frac{1}{1+\kappa\varpi\lambda\Omega_{LI}\theta_2\left(1+T_p^{\alpha}\right)}\right], \quad (38)$$

$$\mathcal{P}_{F_n}^{HD,\infty} \approx \eta_n^2 \sum_{q=1}^{Q}\sum_{q1=1}^{Q}\xi_q^n\xi_{q1}^n\frac{\left(1+T_q^{\alpha}\right)\left(1+T_{q1}^{\alpha}\right)\varsigma_1^*\tau_1^*}{\lambda\rho^2}. \quad (39)$$

Remark 2: Similarly, after substituting (38) and (39) into (35), we can obtain $d_{F_n}^{FD} = 1$ and $d_{F_n}^{HD} = 2$, respectively. Regarding to far user F_n, one diversity gain is obtained for FD NOMA scheme, while the diversity order in HD NOMA is equal to two. Therefore, with the aid of the direct link transmission, the zero diversity gain problem inherent to FD cooperative scheme is thus overcame [18], [29]. One possible reason is that the direct link provides another transmission possibility for the source to communicate with F_n.

3) THE FAR USER F_M

Using (31) and (33), the asymptotic outage probabilities of F_m for FD/HD-based NOMA system at high SNR region are obtained respectively as

$$\mathcal{P}_{F_m}^{FD,\infty} \approx \eta_m \sum_{p=1}^{P}\sum_{q2=1}^{Q}\zeta_p\xi_{q2}^m\frac{\left(1+T_{q2}^{\alpha}\right)\theta_2}{\rho} \times \left[1-\frac{1}{1+\kappa\varpi\lambda\Omega_{LI}\theta_2\left(1+T_p^{\alpha}\right)}\right], \quad (40)$$

$$\mathcal{P}_{F_m}^{HD,\infty} \approx \eta_m^2 \sum_{q2=1}^{Q}\sum_{q3=1}^{Q}\xi_{q2}^m\xi_{q3}^m\frac{\left(1+T_{q2}^{\alpha}\right)\left(1+T_{q3}^{\alpha}\right)\theta_2^*\theta_3^*}{\lambda\rho^2}. \quad (41)$$

Remark 3: Substituting (40) and (41) into (35), it is easy to find $d_{F_m}^{FD} = 1$ and $d_{F_m}^{HD} = 2$, respectively. As the same as the far user F_n, the zero diversity gain limitation of user F_m in FD NOMA is overcame. In fact, even though the performance of the relaying link is still affected by LI, the direct link transmission leads to a nonzero diversity order for F_m in FD NOMA scheme.

C. THROUGHPUT ANALYSIS

In the following, we analyze the system throughput for FD/HD-based NOMA scheme under delay-limited transmission mode in which the base station transmits signals with constant rates $\mathcal{R}_i$, $i \in \{k, m, n\}$ [9], [18]. Recall that γ_{thi} denotes SNR threshold, the signals are decoded successfully if the SINRs at the receiving end are greater than the corresponding threshold γ_{thi}. Therefore, the system throughput in delay-limited mode can be easily obtained, on the basis of the evaluated outage probabilities and the fixed transmission rates.

1) FD-BASED NOMA CASE

Leveraging the analytical results of outage probability in (16), (25) and (31), the throughput of FD NOMA cooperative network in the delay-limited transmission mode is obtained as

$$\mathcal{R}^{FD} = \left(1-\mathcal{P}_{N_k}^{FD}\right)\mathcal{R}_k + \left(1-\mathcal{P}_{F_n}^{FD}\right)\mathcal{R}_n + \left(1-\mathcal{P}_{F_m}^{FD}\right)\mathcal{R}_m. \quad (42)$$

2) HD-BASED NOMA CASE

Likewise, based on the analytical results (21), (28) and (33), the throughput of HD-based NOMA cooperative scheme in the delay-limited transmission mode is given by

$$\mathcal{R}^{HD} = \left(1-\mathcal{P}_{N_k}^{HD}\right)\mathcal{R}_k + \left(1-\mathcal{P}_{F_n}^{HD}\right)\mathcal{R}_n + \left(1-\mathcal{P}_{F_m}^{HD}\right)\mathcal{R}_m. \quad (43)$$

D. HYBRID FULL/HALF DUPLEX COOPERATIVE NOMA

Despite the tremendous advance in LI cancellation techniques has been improved, it is difficult for the FD scheme to always outperform the HD mode. In this case, a practical opportunistic FD/HD relaying network combined with power adaption is devised in [30] to improve a dual-hop cooperative network performance, where the power adaption scheme is based on the concept in [31]. Further in [32], since the existence of residual self-interference degrades outage behavior of one-way FD cooperative scheme, a hybrid one-way FD/two-way

HD relaying system is proposed. Afterwards, the application of NOMA to a hybrid HD/FD relaying scheme is introduced in [33], and it is verified that the hybrid scheme is superior to conventional NOMA, pure HD cooperative NOMA and pure FD cooperative NOMA scheme.

Inspired by the aforementioned works, we propose a cooperative NOMA scheme with hybrid FD/HD user-assisted relaying for further improving outage performance. Because of imperfect LI cancellation mechanism, our FD cooperative NOMA system suffers severe LI in the high SNR regime. Therefore, we attempt to develop a hybrid FD/HD mode by dynamically selecting appropriate mode according to the level of SNR. In other words, the FD mode is used when the level of SNR is less than a predefined SNR threshold $\rho_{\mathcal{U}}$, otherwise HD operation is employed.

To begin with, the outage probability with hybrid relaying mode is expressed as follows:

$$\begin{aligned}\mathcal{P}_{\mathcal{U}}^{Hybrid} &= \min\left\{\mathcal{P}_{\mathcal{U}}^{HD}, \mathcal{P}_{\mathcal{U}}^{FD}\right\} \\ &= \begin{cases}\mathcal{P}_{\mathcal{U}}^{FD}, & with\ \rho < \rho_{\mathcal{U}} \\ \mathcal{P}_{\mathcal{U}}^{HD}, & with\ \rho \geq \rho_{\mathcal{U}},\end{cases}\end{aligned} \tag{44}$$

where $\mathcal{U} \in \{N_k, F_m, F_n\}$.

Further, we aim to determine the switching boundary between two relaying modes for each user. With the aid of outage probabilities deduced in previous part, the analytical value of $\rho_{\mathcal{U}}$ can be calculated in the following.

Proposition 1: For the near user N_k, the FD mode is superior to the HD mode if $\rho < \rho_{N_k}$,

$$\rho_{N_k} = \frac{\sum_{p=1}^{P} \omega_p \sqrt{1-\phi_p^2}\left(\phi_p+1\right)\left(1+T_p^{\alpha}\right)\theta_1^*}{\sum_{p=1}^{P} \omega_p \sqrt{1-\phi_p^2}\left(\phi_p+1\right)\left[1-\frac{1}{1+\kappa\varpi\lambda\Omega_{LI}\theta_1\left(1+T_p^{\alpha}\right)}\right]}. \tag{45}$$

Otherwise, the HD mode is preferred over the FD mode if $\rho \geq \rho_{N_k}$.

Proof: According to (16) and (21), the switching boundary of N_k can be calculated by solving the equality $\mathcal{P}_{N_k}^{FD} = \mathcal{P}_{N_k}^{HD}$. In order to simplify the analysis, a compact solution of ρ_{N_k} can be approximated by letting $P_{N_k}^{FD,\infty} = P_{N_k}^{HD,\infty}$. It is worth to note that simulation results later in Fig. 2 will show that the approximate solution of $\mathcal{P}_{N_k}^{FD,\infty} = \mathcal{P}_{N_k}^{HD,\infty}$ approaches ρ_{N_k}. This is because the asymptotic analysis results and exact analytical results match well in the medium and high SNR region. ■

The following proposition presents the switching value of SNR for the far user F_n.

Proposition 2: As for the far user F_n, the FD mode is preferred to the HD mode if $\rho < \rho_{F_n}$,

$$\rho_{F_n} = \frac{\eta_n^2 \sum_{q=1}^{Q}\sum_{q1=1}^{Q} \xi_q^n \xi_{q1}^n \left(1+T_q^{\alpha}\right)\left(1+T_{q1}^{\alpha}\right)\varsigma_1^*\tau_1^*}{\eta_n \sum_{p=1}^{P}\sum_{q=1}^{Q} \zeta_p \xi_q^n \left(1+T_q^{\alpha}\right)\lambda\varsigma_1\left[1-\frac{1}{1+\kappa\varpi\lambda\Omega_{LI}\theta_2\left(1+T_p^{\alpha}\right)}\right]}. \tag{46}$$

Otherwise, the HD mode outperforms the FD one.

Proof: Similar to the proof in Proposition 1, the switching boundary of F_n can be obtained by solving ρ_{F_n} from the equation $\mathcal{P}_{F_n}^{FD,\infty} = \mathcal{P}_{F_n}^{HD,\infty}$ for which $\mathcal{P}_{F_n}^{FD,\infty}$ and $\mathcal{P}_{F_n}^{HD,\infty}$ are presented respectively in (38) and (39). ■

As such, we can obtain the value of ρ_{F_m} in the following proposition.

Proposition 3: For the far user F_m, the HD mode is inferior to the FD mode if $\rho < \rho_{F_m}$,

$$\rho_{F_m} = \frac{\eta_m^2 \sum_{q2=1}^{Q}\sum_{q3=1}^{Q} \xi_{q2}^m \xi_{q3}^m \left(1+T_{q2}^{\alpha}\right)\left(1+T_{q3}^{\alpha}\right)\theta_2^*\theta_3^*}{\eta_m \sum_{p=1}^{P}\sum_{q2=1}^{Q} \zeta_p \xi_{q2}^m \left(1+T_{q2}^{\alpha}\right)\lambda\theta_2\left[1-\frac{1}{1+\kappa\varpi\lambda\Omega_{LI}\theta_2\left(1+T_p^{\alpha}\right)}\right]}. \tag{47}$$

Otherwise, the HD mode outperforms the FD one.

Proof: Along the lines of the proof in Proposition 2, we let $\mathcal{P}_{F_m}^{FD,\infty} = \mathcal{P}_{F_m}^{HD,\infty}$. Further, using the formulas (40) and (41), the switching boundary in (47) is attained. ■

On the basis of above analysis, three different mode switch thresholds can be obtained.[6] Particularly, for a given SNR level, each user will feed back only one bit of its mode selection message to the base station for making the decision. To be specific, the one-bit feedback will return 1 on full-duplex mode, or 0 when selecting the half-duplex operation. Furthermore, making use of the majority rule [34], our scheme can automatically select a proper mode based on switching boundaries. Accordingly, the proposed scheme could be applied to some distinctive networks, such as Internet of Things (IoT) systems or distributed networks, in which each of terminals may have different requirements to guide reliable transmission.

V. ERGODIC ACHIEVABLE RATE

The ergodic capacity analysis is introduced in this section. In the case of delay-tolerant transmission mode, the source can transmit at arbitrary rates [9], [18]. Accordingly,

[6] Intuitively, the outage behavior will be deteriorated when imperfect SIC is considered. Accordingly, applying our analysis of mode switch thresholds for imperfect SIC scheme is not straightforward and deserves further modifications. Necessarily, we should mention that extension of our analysis to the case of SIC imperfections and study how to design robust hybrid FD/HD scheme to mitigate the negative effects of imperfect SIC will be valuable directions in future works.

the ergodic capacity is an important performance metric for evaluating the maximum transmission rate of a system. Thus, the expressions for the ergodic rate of each user and the ergodic sum rate of FD/HD NOMA systems are derived, respectively. As commonly done in [6] and [7], the ergodic rate of each user can be obtained by calculating the mean value of achievable end-to-end rate.

1) THE NEAR USER N_K

Assuming that the signals x_n and x_m can be detected successfully at the user N_k, then the achievable rate of the user N_k is written as

$$\mathcal{R}_{N_k} = B\log_2\left(1+\gamma_{N_k}\right), \tag{48}$$

where in FD mode B is 1 and $1/2$ for HD operation due to the spectral loss.

Theorem 4: The ergodic achievable rate of the user N_k for FD NOMA system is expressed by

$$C_{N_k}^{FD} = \sum_{p=1}^{P} \frac{\varsigma_p a_k \rho}{\ln 2\left(a_k\rho - \rho_R N_p\right)} \left\{ -e^{\frac{\left(1+T_p^{\alpha}\right)}{a_k\rho}} Ei\left[-\frac{\left(1+T_p^{\alpha}\right)}{a_k\rho}\right] + e^{\frac{1}{\kappa\varpi\rho_R\Omega_{LI}}} Ei\left[-\frac{1}{\kappa\varpi\rho_R\Omega_{LI}}\right]\right\}, \tag{49}$$

in which $N_p = \kappa\varpi\Omega_{LI}\left(1+T_p^{\alpha}\right)$, and $Ei(\cdot)$ is the exponential integral function [28].

Proof: See Appendix D. ■

Corollary 8: Particularly, the ergodic achievable rate of user N_k for HD NOMA scheme is presented as follows:

$$C_{N_k}^{HD} = -\sum_{p=1}^{P} \frac{\varsigma_p}{2\ln 2} e^{\frac{\left(1+T_p^{\alpha}\right)}{a_k\rho}} Ei\left[-\frac{\left(1+T_p^{\alpha}\right)}{a_k\rho}\right]. \tag{50}$$

2) THE FAR USER F_N

In this subsection, note that x_n should be decoded at both user N_k and F_m for SIC process, meanwhile, we assume that user F_n can successfully detect its own message x_n. Thus the achievable rate for user F_n is written as follows

$$\mathcal{R}_{F_n} = B\log_2\left[1+\underbrace{\min\left(\gamma_{F_n\to N_k}, \gamma_{S,F_n\to F_m}, \gamma_{R,F_n\to F_m}, \gamma_{F_n}\right)}_{\Theta}\right]. \tag{51}$$

Thus, the corresponding ergodic rate is given by

$$C_{F_n} = \mathbb{E}\left[B\log_2\left(1+\Theta\right)\right] = \frac{B}{\ln 2}\int_0^{\infty} \frac{1-F_{\Theta}(x)}{1+x}dx, \tag{52}$$

where $F_{\Theta}(x)$ is the CDF of Θ. Clearly, it is challenging to obtain an exact expression of $F_{\Theta}(x)$. In this situation, we resort to the approximation of ergodic rate on the high SNR region, which keeps consistence with the work in [18].

Accordingly, under the case of high SNR regime, i.e., $\rho \to \infty$, we have

$$\lim_{\rho\to\infty} \Theta = \underbrace{\min\left\{\frac{a_n\left|g_{SN_k}\right|^2}{\left(1-a_n\right)\left|g_{SN_k}\right|^2 + \kappa\varpi\lambda|g_{LI}|^2}, \frac{a_n}{1-a_n}, \frac{b}{1-b}\right\}}_{\Theta_N}, \tag{53}$$

and

$$F_{\Theta_N}(x) = 1 - \Pr\left(\left|g_{SN_k}\right|^2 > \frac{\kappa\varpi\lambda|g_{LI}|^2}{a_n-\left(1-a_n\right)x}\right) \times U\left[\min\left(\frac{a_n}{1-a_n}, \frac{b}{1-b}\right) - x\right], \tag{54}$$

where $U(x)$ is unit step function, in which $U(x) = 1$ for $x \geq 1$, otherwise $U(x) = 0$.

Theorem 5: In high SNR regime, the asymptotic ergodic rate of user F_n for FD NOMA scheme is presented as follows:

$$C_{F_n}^{FD} \simeq \sum_{p=1}^{P} \frac{\varsigma_p}{\ln 2}\frac{1}{1-\lambda N_p}\left\{\ln\left(1+\Gamma\right) - \frac{\lambda a_n N_p}{N_p-1+a_n}\ln\left[1+\frac{\left(\lambda N_p-1+a_n\right)\Gamma}{a_n}\right]\right\}, \tag{55}$$

in which $\Gamma \triangleq \min\left(\frac{a_n}{1-a_n}, \frac{b}{1-b}\right)$.

Proof: See Appendix E. ■

Corollary 9: As for HD NOMA network, a high SNR approximation of ergodic rate for user F_n is given by

$$C_{F_n}^{HD} \simeq \frac{1}{2\ln 2}\ln\left(1+\Gamma\right). \tag{56}$$

3) THE FAR USER F_M

Similarly with the analysis of user F_n, the achievable rate of user F_m can be given by

$$\mathcal{R}_{F_m} = B\log_2\left[1+\min\left(\gamma_{F_m\to N_k}, \gamma_{F_m}\right)\right]. \tag{57}$$

Furthermore, the corresponding ergodic rate of F_m in FD NOMA scheme is expressed in the following theorem.

Theorem 6: The asymptotic ergodic rate of F_m for FD NOMA scheme in the high SNR regime is given by

$$C_{F_m}^{FD} \simeq \sum_{p=1}^{P} \frac{\varsigma_p}{\ln 2}\frac{1}{a_m+a_k-\lambda N_p} \times\left[\left(a_m+a_k\right)\ln\left(1+\frac{a_m}{a_k}\right) - \frac{a_m\lambda N_p}{\lambda N_p-a_k}\ln\left(1+\frac{\lambda N_p-a_k}{a_k}\right)\right]. \tag{58}$$

Proof: See Appendix F. ■

Corollary 10: For the special case $\varpi = 0$, i.e., the HD NOMA scheme, the ergodic rate of F_m in the high SNR regime

can be approximated by

$$C_{F_m}^{HD} \simeq \frac{1}{2\ln 2} \ln\left(1+\frac{a_m}{a_k}\right). \tag{59}$$

4) SLOPE ANALYSIS

Aiming to provide further insights, the slope analysis of the ergodic rate for FD/HD NOMA scheme is characterized. As mentioned in [18], the slope value in the high SNR region can be denoted as

$$s_{\mathcal{U}} \triangleq \lim_{\rho\to\infty} \frac{C_{\mathcal{U}}}{\log_{10}\rho}, \tag{60}$$

in which $\mathcal{U} \in \{N_k, F_m, F_n\}$.

a) The near user N_k: To gain more insights, we first rewrite eqs (49) and (50) in simple forms for large SNRs. By using the approximations $e^x \approx 1$ and $Ei(-x) \approx \ln(x) + c$ (c is Euler constant [28]) when $x \to 0$, then (49) and (50) can be simplified in the high-SNR region as

$$C_{N_k}^{FD,\infty} = \sum_{p=1}^{P} \frac{\varsigma_p a_k}{\ln 2\left(a_k - \lambda N_p\right)} \left\{ -\left[\ln\left(\frac{1+T_p^{\alpha}}{a_k\rho}\right)+c\right] + \left[\ln\left(\frac{1}{\kappa\varpi\lambda\rho\Omega_{LI}}\right)+c\right]\right\}, \tag{61}$$

$$C_{N_k}^{HD,\infty} = -\sum_{p=1}^{P} \frac{\varsigma_p}{2\ln 2}\left[\ln\left(\frac{1+T_p^{\alpha}}{a_k\rho}\right)+c\right]. \tag{62}$$

Accordingly, after substituting (61) and (62) into (60), we have $s_{N_k}^{FD} = 0$ and

$$s_{N_k}^{HD} = \lim_{\rho\to\infty} \frac{-\sum_{p=1}^{P} \frac{\varsigma_p}{2\ln 2}\left[\ln\left(\frac{1+T_p^{\alpha}}{a_k\rho}\right)+c\right]}{\log_{10}\rho} = \frac{\ln 10}{2\ln 2} \approx 1.661, \tag{63}$$

where $\sum_{p=1}^{P} \varsigma_p = 1$ can be easily proofed [26].

b) The far user F_n: Based on the analysis in Theorem 5, after substituting (55) and (56) into (60), we can learn that $s_{F_n}^{FD} = s_{F_n}^{HD} = 0$.

c) The far user F_m: Similarly, by substituting the high-SNR approximations from (58) and (59) into (60), we can easily obtain $s_{F_m}^{FD} = s_{F_m}^{HD} = 0$.

Remark 4: On the basis of above analysis, we can observe that $s_{N_k}^{FD} = s_{F_n}^{FD} = s_{F_m}^{FD} = 0$. Take user N_k as an example, when $\rho \to \infty$, the SINR in (4) can be approximated as $\lim_{\rho\to\infty} \gamma_{N_k} = \frac{a_k|g_{SN_k}|^2}{\kappa\varpi\lambda|g_{LI}|^2}$, which is not related with ρ. Accordingly, the ergodic achievable rate of each user in FD NOMA system will converge to a stable value, meanwhile, the ergodic rate ceiling will occur in the high SNR region [18]. On the one hand, this is due to the existence of residual LI in FD relaying system, which limits the performance of the whole network. On the other hand, as for DF relaying system, the ergodic rates for far users mainly depend on the minimum achievable rates, although the direct links exist.

Remark 5: Note that the residual LI does not exist in the HD NOMA scheme, we can draw that $s_{N_k}^{HD} > s_{F_n}^{HD} = s_{F_m}^{HD} = 0$. According to (4) and (48), the ergodic rate for user N_k continues to grow in high SNR regime, as $\gamma_{N_k} = a_k\rho|g_{SN_k}|^2$ is linearly associated with ρ. In addition, the ergodic rate ceilings for far users will occur, along with the continuous growth of ρ [18].

5) ERGODIC SUM RATE

In delay-tolerant transmission mode, the signal received from base station can be buffered at the receiving end. Based on the previous analysis in (49), (55) and (58), the ergodic sum rate of FD NOMA system can be approximated by

$$C_{sum}^{FD} = C_{N_k}^{FD} + C_{F_n}^{FD} + C_{F_m}^{FD}. \tag{64}$$

Similarly, the ergodic capacity for HD NOMA scheme can be obtained, on the basis of (50), (56) and (59), as follows:

$$C_{sum}^{HD} = C_{N_k}^{HD} + C_{F_n}^{HD} + C_{F_m}^{HD}. \tag{65}$$

VI. THE EFFECT OF IMPERFECT CSI

Considering the fact that perfect CSI (pCSI) is complicated to acquire, it cannot be ignored that the channel estimation error can significantly affect the system performance. As a result, we also present a concise analytical analysis under imperfect CSI (ipCSI) scenario for comparison. Accordingly, inspired by the channel estimation model in [35], the channel coefficient can be modeled as $g_{ij} = \widehat{g}_{ij} + \widehat{e}_{ij}$, in which $\widehat{g}_{ij} \triangleq \frac{h_{ij}}{\sqrt{1+d_{ij}^{\alpha}}}$ denotes the estimated channel coefficient and $\widehat{e}_{ij} \triangleq \frac{e_{ij}}{\sqrt{1+d_{ij}^{\alpha}}}$ represents the corresponding channel estimation error. As for instance in [35], e_{ij} is subjected to complex Gaussian distribution with mean zero and the variance σ_e^2, and $\hat{h}_{ij} \sim CN\left(0, 1-\sigma_e^2\right)$. Besides, the un-correlation of $\hat{h}_{ij}$ and e_{ij} is also assumed here.

Due to imperfect CSI, an error term $\rho\left|\widehat{e}_{SN_k}\right|^2$ is introduced to the denominators of eqs (2), (3) and (4). Then, recalling the analysis in (15), the outage probability of user N_k under imperfect CSI can be calculated as

$$\widehat{P}_{N_k}^{FD} \approx 1 - \frac{\rho\tilde{\sigma}_e^2 e^{-\frac{\left(1+\bar{d}_{SN_k}^{\alpha}\right)\theta_1}{\rho\tilde{\sigma}_e}}}{\left(\sigma_e^2\theta_1+\tilde{\sigma}_e\right)\left[\kappa\varpi\rho_R\Omega_{LI}\theta_1\left(1+\bar{d}_{SN_k}^{\alpha}\right)+\rho\tilde{\sigma}_e\right]}, \tag{66}$$

in which $\tilde{\sigma}_e = 1-\sigma_e^2$. Besides, for the sake of mathematical tractability, the results in (66) is approximated by using the mean value of d_{SN_k}, $\bar{d}_{SN_k}$, to replace with d_{SN_k} in $\widehat{g}_{SN_k}$ and $\widehat{e}_{SN_k}$.

Meanwhile, regarding to far users F_n and F_m, the SINRs in (5), (6) and (7) can be further modified with the assumption of imperfect CSI. However, note that

the ordered distance variable $\tilde{d}_{SF_l}$ is related to $\widehat{g}_{SF_l}$ and $\widehat{e}_{SF_l}$, which increases the difficulty of derivation. Similarly, by using the expectation value of $\tilde{d}_{SF_l}$, $\bar{d}_{SF_l}$, we can obtain the following closed-form approximated expressions. In particular, $\bar{d}_{SF_l} = \int_{R_f}^{R_F} r f_{\tilde{d}_{SF_l}}(r)\, dr \approx \frac{C_l (R_F - R_f)}{\left(R_F^2 - R_f^2\right)^C} \sum_{q=1}^{Q} w_Q \sqrt{1-\phi_q^2}\, T_q^2 \left(T_q^2 - R_f^2\right)^l \left(R_F^2 - T_q^2\right)^{C-l}$.

Thus, based on the derived process in Theorem 2, the outage probability of F_n under imperfect CSI can now be expressed as

$$\widehat{P}_{F_n}^{FD} \approx \left(1 - \widehat{P}_{Ai}\right)\left[1 - \frac{\tilde{\sigma}_e}{\left(\sigma_e^2 \varsigma_1 + \tilde{\sigma}_e\right)} e^{-\frac{\left(1+\bar{d}_{SF_n}^{\alpha}\right)\varsigma_1}{\rho\tilde{\sigma}_e}}\right] + \widehat{P}_{Ai}\left[1 - \frac{\tilde{\sigma}_e}{\left(\sigma_e^2 \varsigma_1 + \tilde{\sigma}_e\right)} e^{-\frac{\left(1+\bar{d}_{SF_n}^{\alpha}\right)\varsigma_1}{\rho\tilde{\sigma}_e}}\right] \times \left[1 - \frac{\tilde{\sigma}_e}{\left(\sigma_e^2 \tau_1 + \tilde{\sigma}_e\right)} e^{-\frac{\left(1+\bar{d}_{N_k F_n}^{\alpha}\right)\tau_1}{\rho_R\tilde{\sigma}_e}}\right], \quad (67)$$

where $\widehat{P}_{Ai} \simeq \frac{\rho\tilde{\sigma}_e^2 e^{-\frac{\left(1+\bar{d}_{SN_k}^{\alpha}\right)\theta_2}{\rho\tilde{\sigma}_e}}}{\left(\sigma_e^2\theta_2 + \tilde{\sigma}_e\right)\left[\kappa\varpi\rho_R\Omega_{LI}\theta_2\left(1+\bar{d}_{SN_k}^{\alpha}\right) + \rho\tilde{\sigma}_e\right]}$.

Furthermore, according to (30) and taking similar steps used in Appendix C, the outage probability of user F_m with imperfect CSI can be given by

$$\widehat{P}_{F_m}^{FD} \approx \left(1 - \widehat{P}_{Ai}\right)\left[1 - \frac{\tilde{\sigma}_e}{\left(\sigma_e^2 \theta_2 + \tilde{\sigma}_e\right)} e^{-\frac{\left(1+\bar{d}_{SF_m}^{\alpha}\right)\theta_2}{\rho\tilde{\sigma}_e}}\right] + \widehat{P}_{Ai}\left[1 - \frac{\tilde{\sigma}_e}{\left(\sigma_e^2 \theta_2 + \tilde{\sigma}_e\right)} e^{-\frac{\left(1+\bar{d}_{SF_m}^{\alpha}\right)\theta_2}{\rho\tilde{\sigma}_e}}\right] \times \left[1 - \frac{\tilde{\sigma}_e}{\left(\sigma_e^2 \theta_3 + \tilde{\sigma}_e\right)} e^{-\frac{\left(1+\bar{d}_{N_k F_m}^{\alpha}\right)\theta_3}{\rho_R\tilde{\sigma}_e}}\right]. \quad (68)$$

Particularly, to have an insight of HD NOMA scenario with imperfect CSI, the similar analysis can be easily addressed. More importantly, other performance metrics such as ergodic capacity are certainly influenced by channel estimation error, but are not shown in this section to keep our paper reasonably concise.

VII. NUMERICAL RESULTS

In this section, numerical results are provided to verify the performance of two kinds of NOMA cooperative schemes, i.e., FD/HD-based relaying NOMA scheme, in terms of outage probability and system throughput and ergodic sum rate. Moreover, the set of parameters are used in the following figures: The power allocation factors are set as: $a_n = 7/16$, $a_m = 5/16$, $a_k = 4/16$ and $b = 3/5$, and $\kappa = 0.5$, $m = 1$, $n = 4$, $C = 4$, $\lambda = 0.5$. As for the target rates, we have $\mathcal{R}_n = 0.2$ BPCU, $\mathcal{R}_m = 0.4$ BPCU and $\mathcal{R}_k = 0.5$ BPCU. The complexity-accuracy tradeoff parameter is $N = 50$. The path loss exponent is $\alpha = 2$ [18]. Also, we set some distance parameters as: $R_N = 2$m, $R_f = 20$m and $R_F = 22$m [9]. All the Monte Carlo simulations are repeated at 10^7 realizations.

TABLE 1. Transmission of HD-OMA and FD-OMA.

	HD-OMA		FD-OMA	
Time slots	$\mathcal{S}$	N_k	$\mathcal{S}$	N_k
1	$x_k[j]$	-	$x_k[j]$	-
2	$x_m[j]$	-	$x_m[j]$	$x_m[j-1]$
3	-	$x_m[j]$	$x_n[j]$	$x_n[j-1]$
4	$x_n[j]$	-		
5	-	$x_n[j]$		

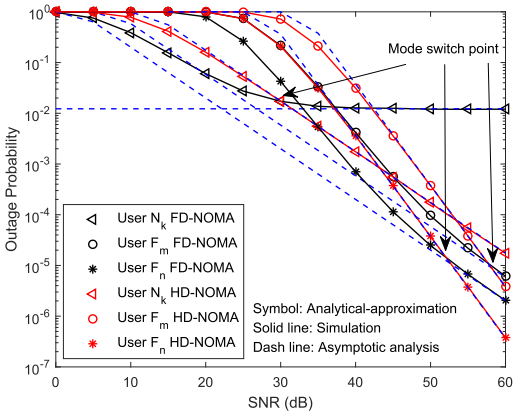

FIGURE 2. Outage probability against the transmit SNR ρ.

A. EXISTING SCHEMES FOR COMPARISON

Without loss of generality, we also take existing schemes as benchmarks to compare [8], [18]. The schemes used for comparison are the FD cooperative NOMA system with/without direct link, the HD cooperative NOMA system with/without direct link, and the OMA-based FD/HD relaying system. Since the expressions for cooperative NOMA system without direct link can be obtained from similar procedures,[7] we only introduce in details the OMA-based relaying system.

To be specific, in OMA-based cooperative scheme [36], [37], we assume that the base station broadcasts the signals x_k, x_m, and x_n using three different time resources, i.e., time division multiple access, respectively. Then, x_m and x_n are forwarded using two orthogonal time slots in N_k-F_i ($i \in \{m, n\}$) link, respectively. Different from the HD-OMA scheme, the user-assisted relaying N_k in OMA-based FD system can transmit and receive information simultaneously. In order to facilitate the analysis, TABLE 1 is introduced to present the transmission process for FD-OMA and HD-OMA. From TABLE 1, we can see that only three orthogonal time slots are required in OMA-based FD scheme, while the total communication process for OMA-based HD scheme is completed using five slots. More importantly, the transmission power of base station in OMA-based

[7]Take user F_n as example, assume that no direct link exists between the far users and base station, the outage probability for FD NOMA scheme of F_n in Eq. (24) can be rewritten as $\mathcal{P}_{F_n}^{FD} = \mathcal{P}_{A_i} \Pr\left(\gamma_{R,F_n} < \gamma_{th_n}^{FD}\right)$. Thus the further derivation can be made in a similar way.

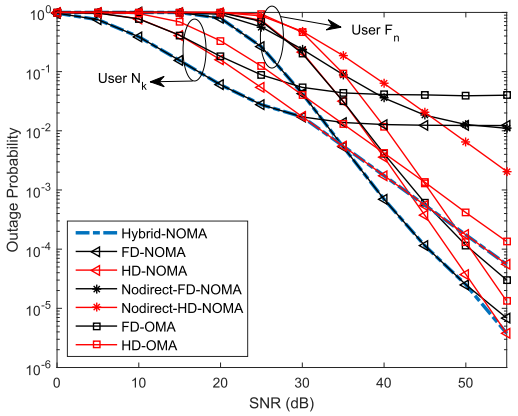

FIGURE 3. Outage probability against the transmit SNR ρ ($\Omega_{LI} = -15$ dB [18]).

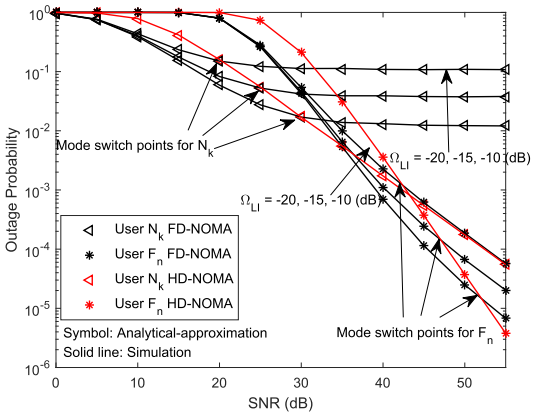

FIGURE 4. Outage probability against the transmit SNR ρ for different values of LI.

scheme should satisfy $P_{O,S} = P_S/3$ for the sake of fairness in total transmission power consumption [37]. Particularly, more details of the performance analysis for FD-OMA and HD-OMA can be seen in Appendix G.

B. OUTAGE PROBABILITY

Fig. 2 shows the variation of the outage probability with transmit SNR ρ under $\Omega_{LI} = -15$ dB [18]. One can observe the perfect agreement between all simulation results and the analytical expressions, and all the asymptotic curves are shown to be tight bounds in the high SNR region. Further, we can observe that by using FD relaying mode, lower outage probability for each user is obtained than that in HD NOMA scheme, particularly in the low-medium SNR region. However, incorporating the effect of residual LI in FD NOMA, observations are drawn as follows: (1) The outage probability of each user in FD NOMA scheme is negatively affected in the high SNR regime; (2) The outage floor of near user N_k exists in the FD-based NOMA scheme, namely the diversity order is zero, which agrees with the conclusion in Remark 1; (3)As for far users F_m and F_n, while leveraging the direct link to convey information, there is no error floor exists in FD NOMA system and one diversity order is obtained, which corroborate the conclusions in Remark 2-3. Consequently, it is reasonable to switch the FD mode only in low and medium SNR region and select the HD operation at high SNR region.

In Fig. 3, we plot the analytical outage performances of users N_k and F_n in the proposed hybrid full/half-duplex NOMA scheme, the FD NOMA system with/without direct link, the HD NOMA system with/without direct link and OMA-based FD/HD relaying scheme. For a fair comparison, all the mentioned schemes have the same target rates $\mathcal{R}_i$, $i \in \{k, m, n\}$, for each user [8]. Firstly, Fig. 3 shows that the hybrid full/half-duplex NOMA scheme for both N_k and F_n has the optimal outage behavior in comparison with the pure FD NOMA and the pure HD NOMA. Secondly, assuming the direct link between F_n and base station is unavailable, user F_n in FD NOMA scheme has zero diversity order loss,

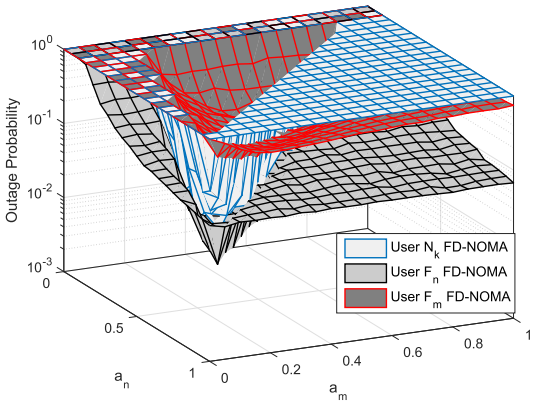

FIGURE 5. Outage probability for FD NOMA scheme versus a_n and a_m ($\rho = 30$ dB, $\Omega_{LI} = -15$ dB).

which illustrates the validity of Remark 2. Another intuitional observation is that, when there exists the direct link for transmission, the performance of the OMA-based FD relaying scheme is inferior to FD cooperative NOMA scheme. Besides, regardless of NOMA or OMA protocol, the outage behavior of FD cooperative scheme exceeds the HD relaying one in the low-medium SNR regime. The result depicts that the effective suppression of loop-interference is required for guaranteeing the advantage of FD transmission mode.

As shown in Fig. 4, the outage behavior of the users N_k and F_n is analyzed versus different values of LI. Considering that the outage probabilities of users F_n and F_m have the similar trend, we only take F_n as example. One can observe that the superior of FD NOMA is confirmed again in the low SNR region. However, with the increase of Ω_{LI} from -20 dB to -10 dB, we can see that, more outage events occur and lead to the advantage brought by FD-based NOMA is not obvious enough. More notably, the mode switch points for each user are shifted to left, as the value of Ω_{LI} is increasing. As a result, the effect of residual LI should be focused enough when leveraging the FD technique into the practical scenario.

Fig. 5 depicts the effect of power allocation factors on outage behavior of near user and far users. Take FD-NOMA

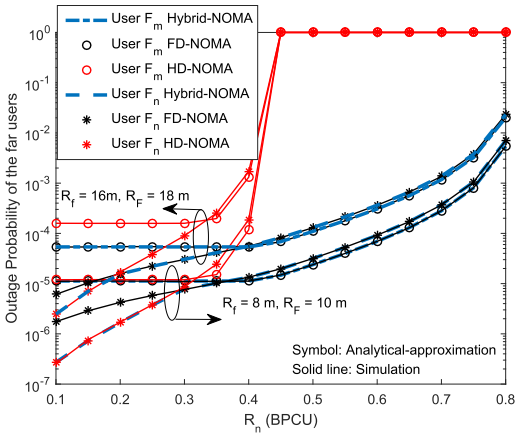

FIGURE 6. Outage probability versus $\mathcal{R}_n$ for different values of radius ($\rho = 40$ dB, $\Omega_{LI} = -15$ dB).

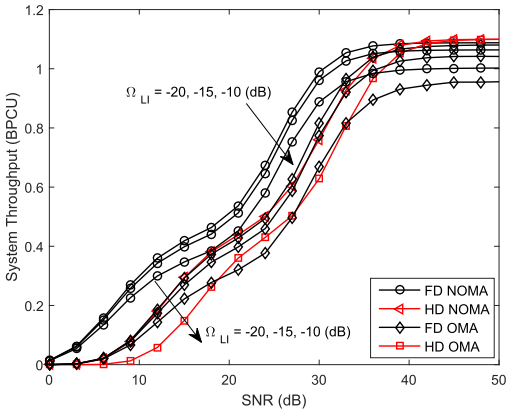

FIGURE 7. System throughput in delay-limited transmission mode against the transmit SNR ρ for different values of LI.

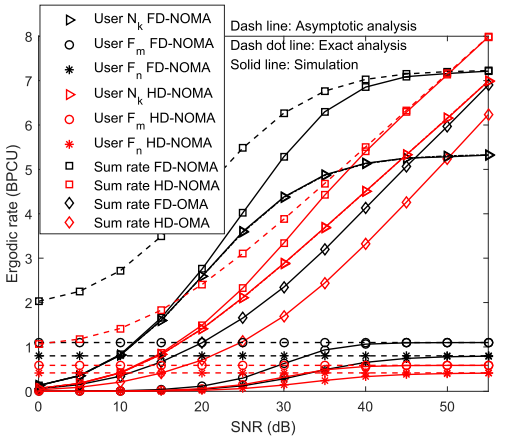

FIGURE 8. Ergodic rate against the transmit SNR ρ ($\Omega_{LI} = -15$ dB).

scheme as example, one can observe that the simulation results can provide a reference on optimal parameter selection. Particularly, if the selected values of a_n and a_m are unreasonable, the outage probability of user N_k will remain at one. The reason is that, according to the SIC process at user N_k, the signals x_n and x_m are required to be decoded first, and then its own signal x_k is decoded. More importantly, the choice of a_n is limited to $a_n - (1 - a_n)\,\gamma_{th_n}^{FD} > 0$, meanwhile, the selection of a_m should satisfy $a_m - a_k\gamma_{th_m}^{FD} > 0$, which are in accordance with the conditions in Theorem 1. However, if the choices of a_n and a_m are correct, a lower outage probability for each far user is obtained by the aid of relay transmission, otherwise, it is mainly determined by the direct link for transmission.

Fig. 6 plots the outage behavior of far users versus the target rate $\mathcal{R}_n$, with different radius R_f and R_F. We see that both the values of radius and target rate can deeply affect the outage performance of far users. Firstly, regarding to FD NOMA system, the outage occurs more frequently with increasing the value of $\mathcal{R}_n$. The reason is that a larger $\mathcal{R}_n$ means a larger decoding threshold for the signal x_n, which may lead to the failure of subsequent decoding and further cause more outage. Secondly, we find that the outage probabilities of HD NOMA scheme will approach one when $\mathcal{R}_n$ becomes larger. This is because based on Eq. (28) and (33), the condition $a_n - (1 - a_n)\,\gamma_{th_n}^{HD} > 0$, which is equivalent to $\mathcal{R}_n < \frac{1}{2}\log_2\left(1 + \frac{a_n}{1-a_n}\right)$, should be met according to NOMA protocol [9]. Thirdly, the larger the value of the radius is, the more likely outage performance of far users is deteriorated. This is due to fact that the far users will have a larger path loss as the distance between BS and each far user increases.

C. SYSTEM THROUGHPUT

Fig. 7 plots the system throughput in delay-limited mode versus transmit SNR with different values of LI from $\Omega_{LI} = -20$ dB to $\Omega_{LI} = -10$ dB. As shown in the figure, it is clear that the FD-based NOMA scheme outperforms HD NOMA system in the low SNR region. As we discussed earlier, the outage probability of FD NOMA is smaller than HD NOMA at the low SNR regime, which leads to a better throughput performance. Furthermore, the growth of the throughput becomes slower with increasing SNR, until the throughput ceilings occur in the high SNR region. The reason is that the outage probabilities are especially small in high SNR regime, so the transmission rates at the base station have held a dominant position in the system throughput. Particularly, another observation is that the throughput of NOMA is superior to OMA scheme in low and medium SNR regions.

D. ERGODIC ACHIEVABLE RATE

Fig. 8 plots the analytical and simulated ergodic rates as a function of transmit SNR. Regarding to user N_k, it reveals that the analytical ergodic rate and simulated result match closely. Also, the simulated ergodic rates for far users converge to their asymptotical values in the high SNR regions. Meanwhile, as the transmit SNR increases, the ergodic rate of user N_k in FD NOMA scheme grows slower until a rate ceiling occurs, while the rate in HD NOMA scheme keeps

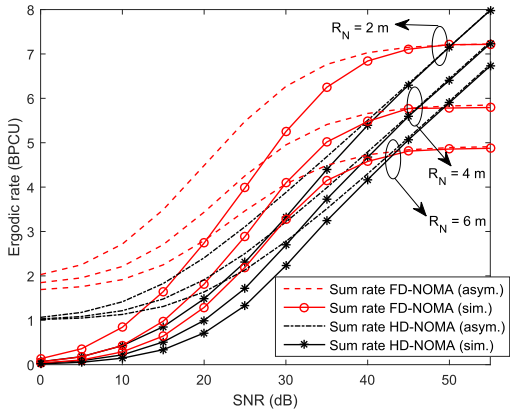

FIGURE 9. Ergodic sum rate against the transmit SNR ρ for different values of R_N ($\Omega_{LI} = -15$ dB).

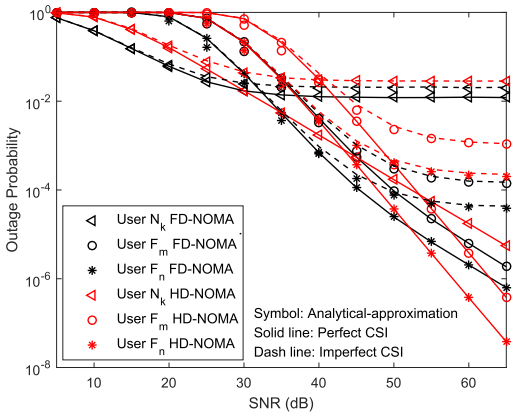

FIGURE 10. Analytical and simulated outage behavior versus transmit SNR ρ with pCSI/ipCSI ($\sigma_e^2 = 0.005$).

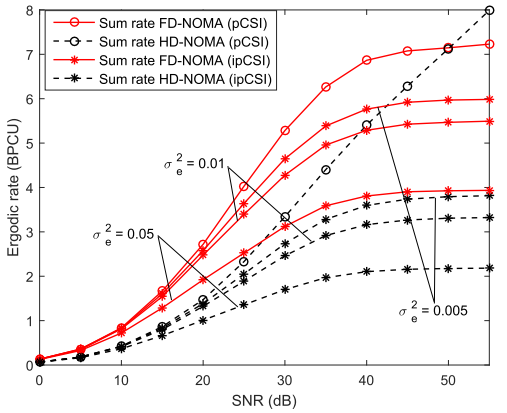

FIGURE 11. Simulated ergodic sum rate versus transmit SNR ρ with pCSI/ipCSI ($\Omega_{LI} = -15$ dB).

improving. Next considering far users, the slopes of these curves in both FD NOMA and HD NOMA at the high SNR region are zero. Both the two conclusions are consistent with the analysis in Remark 4 and 5. More notably, there is a big rate gap between cell-center and cell-edge users at the high SNR region. One possible reason is that the ergodic rate for far user in DF relaying scheme is determined by the minimum achievable rate, although with the direct link for transmission. In terms of ergodic sum rate, the FD NOMA cooperative scheme shows better performance improvement in comparison with the HD NOMA one at low and medium SNR region, i.e., $\rho \leq 50dB$, and vice-versa as the high SNR regime, i.e., $\rho > 50dB$. This is due to the fact that, on the one hand, the application of FD relaying is beneficial when the transmit SNR is relatively small, while the HD NOMA scheme suffers transmission time loss. On the other hand, the FD NOMA scheme loses it advantage in high SNR region as the effect of LI is more severe.

In Fig. 9, we examine the effect of radius R_N on the performance of the proposed scheme in terms of ergodic sum rate. Obviously, it can be seen that the ergodic sum rates of both HD NOMA and FD NOMA are greatly improved with decreasing of R_N, which indicates that the impact of path-loss degradation is significant. To be specific, there is a high probability of selecting a near user with better channel condition, since more near users are located closer to the base station. As shown previously in Fig. 8, the ergodic rates of far users limit the ergodic capacity of the whole network in the high SNR region. Consequently, the appropriate choice of radius R_N is required for enhancing ergodic sum rate of the considered system.

E. IMPACT OF CSI IMPERFECTIONS

Fig. 10 and Fig. 11 plot outage behavior and ergodic sum rate for both FD and HD NOMA schemes in the presence of channel estimation error, respectively. The results in Fig. 10 present the agreement in the high SNR regime between the analytical analysis (as given in (66)-(68)) and the simulated results. One observation is that, when the imperfection in CSI is considered, the outage behavior in both FD and HD schemes deteriorates and then reaches the fixed values. Besides, the error floor phenomenon happens, meanwhile, the diversity orders go to zero for the reason of the error in channel estimation. Moreover, due to the effect of CSI imperfection, we can see that FD NOMA outperforms HD NOMA in terms of outage behavior and ergodic capacity. In Fig. 11, we depict the simulated ergodic capacity in the case of both perfect and imperfect CSI. As it is obvious, as the increase of the transmit SNR, the ergodic sum rates under different values of σ_e^2 keep improve but reach different rate ceilings. Further, it can be drawn that the ergodic capacity in both FD NOMA and HD NOMA schemes deteriorates with the increasing of error variance. Therefore, the channel estimation error has a strong affect on the system performance, which should be paid more attention at the practical application.

VIII. CONCLUSION

In this paper, the performance analysis of the FD/HD user-assisted relaying in cooperative NOMA scheme has been studied in terms of outage probability, system throughput and ergodic sum rate. We have also taken the impact of the location of user into consideration on the system performance. Furthermore, due to the effect of residual LI, the near user achieves zero diversity order inherent to the

FD mode, whereas far users obtain one diversity order by exploiting the direct link transmission. Based on the analytical results for outage behavior, delay-limited throughput and ergodic sum rate, we can conclude that the FD-based NOMA system is superior to the HD NOMA scheme in the lower SNR region. In addition, the advantage of FD operation is not pronounced enough with the increase of LI. Thus the outage behavior is further improved by a hybrid FD/HD relaying scheme which can select the proper mode according to different SNR levels. The numerical results verify the accuracy of our analytical results.

In the future, extending this work for multiple antennas cooperative NOMA scheme is one significant direction to pursue, and the more realistic problems such as SIC imperfections [38] and other important user selection methods [9] may deserve consideration.

APPENDIX A
PROOF OF COROLLARY 1

Firstly, equation (12) can be rewritten as

$$f_{\tilde{d}_{SF_l}}(r) = C_l \frac{2r\left(r^2 - R_f^2\right)^{l-1}\left(R_F^2 - r^2\right)^{C-l}}{\left(R_F^2 - R_f^2\right)^{C}}. \quad \text{(A.1)}$$

Further, for the special case $\alpha = 2$, substituting (A.1) into (9) and defining $t = r^2 - R_f^2$, $F_{|g_{SF_l}|^2}$ can be written as

$$\begin{aligned} &F_{|g_{SF_l}|^2} \\ &= \int_0^{R_F^2 - R_f^2} \left(1 - e^{-\left(1+R_f^2+t\right)x}\right) \frac{C_l t^{l-1}\left(R_F^2 - R_f^2 - t\right)^{C-l}}{\left(R_F^2 - R_f^2\right)^{C}} dt \\ &\overset{\langle a \rangle}{=} \sum_{p=0}^{C-l} \binom{C-l}{p} \frac{C_l(-1)^p}{\left(R_F^2 - R_f^2\right)^{l+p}} \left[\int_0^{R_F^2 - R_f^2} t^{l+p-1}\, dt \right. \\ &\quad \left. - e^{-\left(1+R_f^2\right)x} \underbrace{\int_0^{R_F^2 - R_f^2} e^{-xt} t^{l+p-1} dt}_{\mathcal{L}} \right], \end{aligned} \quad \text{(A.2)}$$

where the step $\langle a \rangle$ is attained by using the binomial theorem.

With the aid of [28, Eq.(3.351.1)], $\mathcal{L}$ can be further calculated as

$$\mathcal{L} = x^{-(l+p)} \gamma\left(l+p, \left(R_F^2 - R_f^2\right)x\right). \quad \text{(A.3)}$$

Lastly, plugging (A.3) into (A.2) and doing some integral calculations, we can obtain (14).

The proof is done.

APPENDIX B
PROOF OF THEOREM 2

Equation (24) can be rewritten as:

$$\begin{aligned} \mathcal{P}_{F_n}^{FD} &= \left(1 - \mathcal{P}_{A_i}\right) \underbrace{\Pr\left(\gamma_{S,F_n} < \gamma_{th_n}^{FD}\right)}_{I_1} \\ &\quad + \mathcal{P}_{A_i} \underbrace{\Pr\left(\gamma_{S,F_n} < \gamma_{th_n}^{FD}, \gamma_{R,F_n} < \gamma_{th_n}^{FD}\right)}_{I_2}. \end{aligned} \quad \text{(B.1)}$$

Further, recalling equation (5), I_1 and I_2 can be rewritten respectively as

$$\begin{aligned} I_1 &= \Pr\left(\left|g_{SF_n}\right|^2 < \frac{\gamma_{th_n}^{FD}}{\rho\left[a_n - (1-a_n)\gamma_{th_n}^{FD}\right]}\right) \\ &= F_{|g_{SF_n}|^2}\left(\frac{\varsigma_1}{\rho}\right), \end{aligned} \quad \text{(B.2)}$$

$$\begin{aligned} I_2 &= \Pr\left(\left|g_{SF_n}\right|^2 < \frac{\varsigma_1}{\rho}, \left|g_{N_k F_n}\right|^2 < \frac{\gamma_{th_n}^{FD}}{\rho_R\left[b - (1-b)\gamma_{th_n}^{FD}\right]}\right) \\ &= F_{|g_{SF_n}|^2}\left(\frac{\varsigma_1}{\rho}\right) F_{|g_{N_k F_n}|^2}\left(\frac{\tau_1}{\rho_R}\right). \end{aligned} \quad \text{(B.3)}$$

Next, recalling the CDFs of $\left|g_{SF_n}\right|^2$ and $\left|g_{N_k F_n}\right|^2$ in Section III, therefore we have

$$\begin{aligned} I_1 \approx C_n \sum_{q=1}^{Q} \omega_Q \sqrt{1-\phi_q^2}\left(R_F - R_f\right)\left[1 - e^{-\frac{\left(1+T_q^\alpha\right)\varsigma_1}{\rho}}\right] \\ \times \frac{T_q\left(T_q^2 - R_f^2\right)^{n-1}\left(R_F^2 - T_q^2\right)^{C-n}}{\left(R_F^2 - R_f^2\right)^{C}}, \end{aligned} \quad \text{(B.4)}$$

and I_2 can be seen in (B.5), as shown at the top of the next page.

Theorem 2 is proofed by plugging (B.4), (B.5) and (23) into (B.1).

APPENDIX C
PROOF OF THEOREM 3

For starters, substituting (6) into (30), J_1 can be rewritten as

$$\begin{aligned} J_1 &= 1 - \Pr\left(g_{|SF_m|^2} > \frac{\theta_2}{\rho}\right) \\ &\approx \eta_m \sum_{q2=1}^{Q} \sqrt{1-\phi_{q2}^2} T_{q2}\left(T_{q2}^2 - R_f^2\right)^{m-1}\left(R_F^2 - T_{q2}^2\right)^{C-m} \\ &\quad \times \left[1 - e^{-\frac{\left(1+T_{q2}^\alpha\right)\theta_2}{\rho}}\right]. \end{aligned} \quad \text{(C.1)}$$

Then substituting (7) into (30), J_2 can be calculated by

$$\begin{aligned} J_2 &= 1 - \Pr\left(g_{|N_k F_m|^2} > \frac{\theta_3}{\rho_R}\right) \\ &\approx \eta_m \sum_{q3=1}^{Q} \sqrt{1-\phi_{q3}^2} T_{q3}\left(T_{q3}^2 - R_f^2\right)^{m-1}\left(R_F^2 - T_{q3}^2\right)^{C-m} \end{aligned}$$

$$I_2 \approx \left[\frac{C_n\omega_Q\left(R_F-R_f\right)}{\left(R_F^2-R_f^2\right)^C}\right]^2 \sum_{q=1}^{Q}\sum_{q1=1}^{Q}\sqrt{\left(1-\phi_q^2\right)\left(1-\phi_{q1}^2\right)}\left[\left(T_q^2-R_f^2\right)\left(T_{q1}^2-R_f^2\right)\right]^{n-1} \times\left[\left(R_F^2-T_q^2\right)\left(R_F^2-T_{q1}^2\right)\right]^{C-n}\left[1-e^{-\frac{\left(1+T_q^\alpha\right)\varsigma_1}{\rho}}\right]\left[1-e^{-\frac{\left(1+T_{q1}^\alpha\right)\tau_1}{\rho_R}}\right] \quad \text{(B.5)}$$

$$\times\left[1-e^{-\frac{\left(1+T_{q3}^\alpha\right)\theta_3}{\rho_R}}\right] \quad \text{(C.2)}$$

At last, combining (23), (C.1) and (C.2), we can obtain (31). The proof is done.

APPENDIX D
PROOF OF THEOREM 4

Based on the achievable rate in (48), the corresponding ergodic rate of N_k is given by

$$C_{N_k}^{FD} = \mathbb{E}\left[\log_2\left(1+\gamma_{N_k}\right)\right] = \frac{1}{\ln 2}\int_0^\infty \frac{1-F_{\gamma_{N_k}}(x)}{1+x}dx, \quad \text{(D.1)}$$

in which $F_{\gamma_{N_k}}(x)$ denotes the CDF of γ_{N_k}.

Next, recalling the expression of γ_{N_k} in (4) and doing some manipulations, its CDF can be derived as follows:

$$F_{\gamma_{N_k}}(x) = \Pr\left(\gamma_{N_k}<x\right) = \int_0^\infty F_{|g_{SN_k}|^2}\left[\frac{(1+\kappa\varpi\rho_R y)\,x}{a_k\rho}\right] f_{|g_{LI}|^2}(y)\,dy = \sum_{p=1}^{P}\varsigma_p\left[1-\frac{a_k\rho e^{-\frac{\left(1+T_p^\alpha\right)x}{a_k\rho}}}{\left(1+T_p^\alpha\right)\kappa\varpi\rho_R\Omega_{LI}x+a_k\rho}\right]. \quad \text{(D.2)}$$

After substituting (D.2) into (D.1), $C_{N_k}^{FD}$ can be further expressed by

$$C_{N_k}^{FD} = \sum_{p=1}^{P}\frac{\varsigma_p}{\ln 2}\int_0^\infty \frac{a_k\rho e^{-\frac{\left(1+T_p^\alpha\right)x}{a_k\rho}}}{(1+x)\left(\rho_R N_p x+a_k\rho\right)}dx = \sum_{p=1}^{P}\frac{\varsigma_p}{\ln 2}\left[\frac{a_k\rho}{a_k\rho-\rho_R N_p}\underbrace{\int_0^\infty \frac{e^{-\frac{\left(1+T_p^\alpha\right)x}{a_k\rho}}}{1+x}dx}_{\Theta_1} - \frac{a_k\rho\rho_R N_p}{a_k\rho-\rho_R N_p}\underbrace{\int_0^\infty \frac{e^{-\frac{\left(1+T_p^\alpha\right)x}{a_k\rho}}}{\rho_R N_p x+a_k\rho}dx}_{\Theta_2}\right]. \quad \text{(D.3)}$$

Moreover, using [28, eq. (3.352.2)], Θ_1 and Θ_2 can be obtained respectively as follows:

$$\Theta_1 = -e^{\frac{\left(1+T_p^\alpha\right)}{a_k\rho}}Ei\left[-\frac{\left(1+T_p^\alpha\right)}{a_k\rho}\right], \quad \Theta_2 = -\left(1/\rho_R N_p\right)e^{\frac{\left(1+T_p^\alpha\right)}{\rho_R N_p}}Ei\left[-\frac{\left(1+T_p^\alpha\right)}{\rho_R N_p}\right]. \quad \text{(D.4)}$$

Finally, after substituting Θ_1 and Θ_2 into (D.3), equation (49) is obtained. The proof is completed.

APPENDIX E
PROOF OF THEOREM 5

Recalling the CDF of Θ_N, equation (54) can be further derived as follows:

$$F_{\Theta_N}(x) = 1-\sum_{p=1}^{P}\varsigma_p\frac{a_n-(1-a_n)\,x}{\lambda N_p x+a_n-(1-a_n)\,x}U\left[\Gamma-x\right]. \quad \text{(E.1)}$$

After substituting (E.1) into (52) and doing some mathematical operations, $C_{F_n}^{FD}$ can be written as

$$C_{F_n}^{FD} \simeq \sum_{p=1}^{P}\frac{\varsigma_p}{\ln 2}\frac{1}{\left(1-\lambda N_p\right)}\int_0^\Gamma \frac{1}{\left(1-\lambda N_p\right)(1+x)} - \frac{\lambda a_n N_p}{\lambda N_p x+a_n-(1-a_n)\,x}dx. \quad \text{(E.2)}$$

Finally, doing some simple integral operations in (E.2), the equation (55) can be obtained. The proof is done.

APPENDIX F
PROOF OF THEOREM 6

To derive the ergodic rate of user F_m, we have

$$C_{F_m}^{FD} = \mathbb{E}\left[\log_2\left(1+\Theta_m\right)\right] = \frac{1}{\ln 2}\int_0^\infty \frac{1-F_{\Theta_m}(x)}{1+x}dx, \quad \text{(F.1)}$$

in which $\Theta_m = \min\left(\gamma_{F_m\to N_k}, \gamma_{F_m}\right)$.

However, it is difficult to obtain the exact expression of $F_{\Theta_m}(x)$. Being consistent with the analysis in user F_n, we only focus on the ergodic rate at the high SNR region. Therefore, when $\rho\to\infty$, $\gamma_{F_m\to N_k}$ and γ_{F_m} can be approximated as $\lim_{\rho\to\infty}\gamma_{F_m\to N_k} = \frac{a_m|g_{SN_k}|^2}{a_k|g_{SN_k}|^2+\kappa\varpi\lambda|g_{LI}|^2}$ and

$\lim_{\rho\to\infty}\gamma_{S,F_m}=\frac{a_m}{a_k}$, respectively. Thus, we let

$$\Theta_M=\min\left[\frac{a_m\left|g_{SN_k}\right|^2}{a_k\left|g_{SN_k}\right|^2+\kappa\varpi\lambda|g_{LI}|^2},\max\left(\frac{a_m}{a_k},\gamma_{R,F_m}\right)\right]. \tag{F.2}$$

Next, denote Λ_1 as $\Pr\left(\frac{a_m\left|g_{SN_k}\right|^2}{a_k\left|g_{SN_k}\right|^2+\kappa\varpi\lambda|g_{LI}|^2}>x\right)$ and Λ_2 as $\Pr\left[\max\left(\frac{a_m}{a_k},\gamma_{R,F_m}\right)>x\right]$, the CDF of Θ_M can be written as

$$F_{\Theta_M}=1-\Lambda_1\Lambda_2. \tag{F.3}$$

Meanwhile, Λ_1 and Λ_2 are given by

$$\Lambda_1=\sum_{p=1}^{P}\varsigma_p\frac{a_m-a_kx}{\lambda N_px+a_m-a_kx}U\left(\frac{a_m}{a_k}-x\right), \tag{F.4}$$

and

$$\Lambda_2=1-\sum_{q2=1}^{Q}\eta_m\xi_{q2}^m\left[1-e^{-\frac{\left(1+T_{q2}^{\alpha}\right)x}{(1-b)\rho_R}}\right]U\left(x-\frac{a_m}{a_k}\right). \tag{F.5}$$

Moreover, substituting (F.4) and (F.5) into (F.3), and based on (F.3), the approximated ergodic rate of F_m can be given by

$$C_{F_m}^{HD}\simeq\frac{1}{\ln 2}\int_0^{\frac{a_m}{a_k}}\left(\frac{M_1}{1+x}+\frac{M_2}{\lambda N_px+a_m-a_kx}\right)dx, \tag{F.6}$$

in which $M_1=\frac{1}{a_m+a_k-\lambda N_p}$ and $M_2=-\frac{\lambda N_pa_m}{a_m+a_k-\lambda N_p}$. After finishing the above integrals and substituting the results into (F.6), we complete the proof.

APPENDIX G
ANALYSIS OF OMA SCHEME

In this part, the expressions for performance of OMA-based HD relaying scheme and OMA-based FD relaying system are presented as follows. Firstly, the base station broadcasts signal x_i, $i\in\{m,n,k\}$, in turn, the SINR for OMA-based cooperative scheme at user N_k to detect x_i, is given by

$$\gamma_{N_k}^{FD/HD}=\frac{P_{O,S}\left|g_{SN_k}\right|^2}{\kappa\varpi P_R|g_{LI}|^2+\sigma^2}, \tag{G.1}$$

where ϖ equals to 1 for the FD mode, and equals to 0 for the HD operation.

Further, the signals x_m and x_n are forwarded to the corresponding far user, respectively. After receiving signals from source and user N_k and merging by selection combining, we can obtain the SINR at far user F_j ($j\in\{m,n\}$) for OMA cooperative scheme, i.e., FD-OMA and HD-OMA, as follows:

$$\gamma_{F_j}^{FD/HD}=\max\left(\frac{P_{O,S}\left|g_{SF_j}\right|^2}{\sigma^2},\frac{P_R\left|g_{N_kF_j}\right|^2}{\sigma^2}\right). \tag{G.2}$$

On the basis of the above analysis, the outage probability for user N_k in HD-OMA and FD-OMA schemes is

$$\mathcal{O}_{N_k}=\Pr\left(\frac{1}{T}\log_2\left(1+\gamma_{N_k}^{FD/HD}\right)<\mathcal{R}_k\right), \tag{G.3}$$

in which T is the required time slots for a total communication process. Also, T is 5 for HD-OMA scheme, otherwise T is 3 in FD-OMA system.

Similar to the analysis in Section III, an outage will occur as follows:(i) F_j can not detect its own information x_j from direct link when N_k fails to decode x_j; (ii) The received SINR after SC at F_j is below its target threshold when x_j can be detected successfully at relaying. As a result, the outage probability for far user F_j is given by

$$\begin{aligned}\mathcal{O}_{F_j}=&\Pr\left[\frac{1}{T}\log_2\left(1+\gamma_{N_k}^{FD/HD}\right)<\mathcal{R}_j\right]\\&\times\Pr\left[\frac{1}{T}\log_2\left(1+\frac{P_{O,S}\left|g_{SF_j}\right|^2}{\sigma^2}\right)<\mathcal{R}_j\right]\\&+\Pr\left[\frac{1}{T}\log_2\left(1+\gamma_{N_k}^{FD/HD}\right)>\mathcal{R}_j\right]\\&\times\Pr\left[\frac{1}{T}\log_2\left(1+\gamma_{F_j}^{FD/HD}\right)<\mathcal{R}_j\right].\end{aligned} \tag{G.4}$$

Meanwhile, the ergodic sum rate of OMA-based cooperative system, i.e., HD-OMA and FD-OMA is presented as:

$$\begin{aligned}C_{OMA}^{FD/HD}=&\frac{1}{T}\mathbb{E}\left[\log_2\left(1+\gamma_{N_k}^{FD/HD}\right)\right]\\&+\sum_j\frac{1}{T}\mathbb{E}\left[\log_2\left\{1+\max\left[\frac{P_{O,S}\left|g_{SF_j}\right|^2}{\sigma^2},\right.\right.\right.\\&\left.\left.\left.\min\left(\gamma_{N_k}^{FD/HD},\frac{P_R\left|g_{N_kF_j}\right|^2}{\sigma^2}\right)\right]\right\}\right].\end{aligned} \tag{G.5}$$

REFERENCES

[1] Q. C. Li, H. Niu, A. T. Papathanassion, and G. Wu, "5G network capcity: Key elements and technologies," *IEEE Veh. Technol. Mag.*, vol. 9, no. 1, pp. 71–78, Mar. 2014.

[2] R. Q. Hu and Y. Qian, "An energy efficient and spectrum efficient wireless heterogeneous network framework for 5G systems," *IEEE Commun. Mag.*, vol. 52, no. 5, pp. 94–101, May 2014.

[3] Z. Ding, M. Peng, and H. V. Poor, "Cooperative non-orthogonal multiple access in 5G systems," *IEEE Commun. Lett.*, vol. 19, no. 8, pp. 1462–1465, Aug. 2015.

[4] L. Dai, B. Wang, and Y. Yuan, S. Han, C.-L. I, and Z. Wang, "Non-orthogonal multiple access for 5G: Solutions, challenges, opportunities, and future research trends," *IEEE Commun. Mag.*, vol. 53, no. 9, pp. 74–81, Sep. 2015.

[5] Z. Ding, Z. Yang, P. Fan, and H. V. Poor, "On the performance of non-orthogonal multiple access in 5G systems with randomly deployed users," *IEEE Signal Process. Lett.*, vol. 21, no. 12, pp. 1501–1505, Dec. 2014.

[6] O. Abbasi, A. Ebrahimi, and N. Mokari, "NOMA inspired cooperative relaying system using an AF relay," *IEEE Wireless Commun. Lett.*, vol. 8, no. 1, pp. 261–264, Feb. 2019.

[7] O. Abbasi and A. Ebrahimi, "Cooperative NOMA with full-duplex amplify- and-forward relaying," *Trans. Emerg. Telecommun. Technol.*, vol. 29, no. 7, p. e3421, Jul. 2018.

[8] J. Men, J. Ge, and C. Zhang, "Performance analysis of non-orthogonal multiple access for relaying networks over Nakagami-*m* fading channels," *IEEE Trans. Veh. Technol.*, vol. 66, no. 2, pp. 1200–1208, Feb. 2017.

[9] Y. Liu, Z. Ding, M. Elkashlan, and H. V. Poor, "Cooperative non-orthogonal multiple access with simultaneous wireless information and power transfer," *IEEE J. Sel. Areas Commun.*, vol. 34, no. 4, pp. 938–953, Apr. 2016.

[10] Z. Zhang, H. Sun, R. Q. Hu, and Y. Qian, "Stochastic geometry based performance study on 5G non-orthogonal multiple access scheme," in *Proc. IEEE Global Commun. Conf. (GLOBECOM)*, Washington, DC, USA, Dec. 2016, pp. 1–6.

[11] Z. Ding, P. Fan, and H. V. Poor, "On the coexistence between full-duplex and NOMA," *IEEE Wireless Commun. Lett.*, vol. 7, no. 5, pp. 692–695, Oct. 2018.
[12] Z. Zhang, Z. Ma, M. Xiao, Z. Ding, and P. Fan, "Full-duplex device-to-device aided cooperative non-orthogonal multiple access," *IEEE Trans. Veh. Technol.*, vol. 66, no. 5, pp. 4467–4471, May 2017.
[13] C. Zhong and Z. Zhang, "Non-orthogonal multiple access with cooperative full-duplex relaying," *IEEE Commun. Lett.*, vol. 20, no. 12, pp. 2478–2481, Dec. 2016.
[14] A. C. M. Austin, O. Afisiadis, and A. Burg, "Digital predistortion of hardware impairments for full-duplex transceivers," in *Proc. IEEE Global Conf. Signal Inf. Process. (GlobalSIP)*, Montreal, QC, Canada, Nov. 2017, pp. 878–882.
[15] E. Foroozanfard, E. De Carvalho, and G. F. Pedersen, "TX-RX isolation method based on polarization diversity, spatial diversity and TX beamforming," in *Proc. Int. Symp. Antennas Propag. (ISAP)*, Okinawa, Japan, Oct. 2016, pp. 34–35.
[16] T. Huusari, Y.-S. Choi, P. Liikkanen, D. Korpi, S. Talwar, and M. Valkama, "Wideband self-adaptive RF cancellation circuit for full-duplex radio: Operating principle and measurements," in *Proc. IEEE 81st Veh. Technol. Conf. (VTC Spring)*, Glasgow, U.K., May 2015, pp. 1–7.
[17] D. Yang and A. Molnar, "A widely tunable active duplexing transceiver with same-channel concurrent RX/TX and 30dB RX/TX isolation," in *Proc. IEEE Radio Freq. Integr. Circuits Symp.*, Tampa, FL, USA, Jun. 2014, pp. 321–324.
[18] X. Yue, Y. Liu, S. Kang, A. Nallanathan, and Z. Ding, "Exploiting full/half-duplex user relaying in NOMA systems," *IEEE Trans. Commun.*, vol. 66, no. 2, pp. 560–575, Feb. 2018.
[19] T. Do *et al.*, "Improving the performance of cell-edge users in NOMA systems using cooperative relaying," *IEEE Trans. Commun.*, vol. 66, no. 5, pp. 1883–1901, May 2018.
[20] L. Zhang, J. Liu, M. Xiao, G. Wu, Y.-C. Liang, and S. Li, "Performance analysis and optimization in downlink NOMA systems with cooperative full-duplex relaying," *IEEE J. Sel. Areas Commun.*, vol. 35, no. 10, pp. 2398–2412, Oct. 2017.
[21] M. F. Kader, M. B. Shahab, and S. Y. Shin, "Non-orthogonal multiple access for a full-duplex cooperative network with virtually paired users," *Comput. Commun.*, vol. 120, pp. 1–9, May 2018.
[22] M. B. Shahab, M. F. Kader, and S. Y. Shin, "A virtual user pairing scheme to optimally utilize the spectrum of unpaired users in non-orthogonal multiple access," *IEEE Signal Process. Lett.*, vol. 23, no. 12, pp. 1766–1770, Dec. 2016.
[23] M. B. Shahab and S. Y. Shin, "Time shared half/full-duplex cooperative noma with clustered cell edge users," *IEEE Commun. Lett.*, vol. 22, no. 9, pp. 1794–1797, Sep. 2018.
[24] D. P. M. Osorio, E. E. B. Olivo, H. Alves, J. C. S. S. Filho, and M. Latva-Aho, "Exploiting the direct link in full-duplex amplify- and-forward relaying networks," *IEEE Signal Process. Lett.*, vol. 22, no. 10, pp. 1766–1770, Oct. 2015.
[25] K. J. Kim, T. Khan, and P. Orlik, "Performance analysis of cooperative systems with unreliable backhauls and selection combining," *IEEE Trans. Veh. Technol.*, vol. 66, no. 3, pp. 2448–2461, Mar. 2017.
[26] F. B. Hildebrand, *Introduction to Numerical Analysis*. New York, NY, USA: Dover, 1987.
[27] H. A. David and H. N. Nagaraja, *Order Statistics*. Hoboken, NJ, USA: Wiley, 1970.
[28] I. S. Gradshteyn and I. M. Ryzhik, *Table of Integrals, Series and Products*. 6th ed. New York, NY, USA: Academic, 2000.
[29] Y. Deng, K. J. Kim, T. Q. Duong, M. Elkashlan, G. K. Karagiannidis, and A. Nallanathan, "Full-duplex spectrum sharing in cooperative single carrier systems," *IEEE Trans. Cogn. Commun. Netw.*, vol. 2, no. 1, pp. 68–82, Mar. 2016.
[30] X. Xia, Y. Xu, K. Xu, W. Ma, and D. Zhang, "Practical opportunistic full-/half-duplex relaying," *IET Commun.*, vol. 9, no. 6, pp. 745–753, Apr. 2015.
[31] K. Xu, D. Zhang, Y. Xu, and W. Ma, "On the equivalence of two optimal power-allocation schemes for A-TWRC," *IEEE Trans. Veh. Technol.*, vol. 63, no. 4, pp. 1970–1976, May 2014.
[32] Y. Wang, K. Xu, A. Liu, and X. Xia, "Hybrid one-way full-duplex/two-way half-duplex relaying scheme," *IEEE Access*, vol. 5, pp. 7737–7745, 2017.
[33] G. Liu, X. Chen, Z. Ding, Z. Ma, and F. R. Yu, "Hybrid half-duplex/full-duplex cooperative non-orthogonal multiple access with transmit power adaptation," *IEEE Trans. Wireless Commun.*, vol. 17, no. 1, pp. 506–519, Jan. 2018.
[34] D. Bubboloni and M. Gori, "Symmetric majority rules," *Math. Social Sci.*, vol. 76, pp. 73–86, Jul. 2015.
[35] F. Fang, H. Zhang, J. Cheng, S. Roy, and V. C. M. Leung, "Joint user scheduling and power allocation optimization for energy-efficient NOMA systems with imperfect CSI," *IEEE J. Sel. Areas Commun.*, vol. 35, no. 12, pp. 2874–2885, Dec. 2017.
[36] X. Liu, Y. Liu, X. Wang, and H. Lin, "Highly efficient 3-D resource allocation techniques in 5G for NOMA-enabled massive MIMO and relaying systems," *IEEE J. Sel. Areas Commun.*, vol. 35, no. 12, pp. 2785–2797, Dec. 2017.
[37] Q. Y. Liau and C. Y. Leow, "Cooperative NOMA system with virtual full-duplex user relaying," *IEEE Access*, vol. 7, pp. 2502–2511, 2019. doi: 10.1109/ACCESS.2018.2886656.
[38] M. B. Shahab and S. Y. Shin, "User pairing and power allocation for non-orthogonal multiple access: Capacity maximization under data reliability constraints," *Phys. Commun.*, vol. 30, pp. 132–144, Oct. 2018.

NINGNING GUO received the B.S. degree from the School of Telecommunication Engineering, Xidian University, Xi'an, China, in 2015, where she is currently pursuing the Ph.D. degree in communication and information system. She is very interested in system design and the performance analysis of wireless communication systems. Her research interests include 5G wireless networks, non-orthogonal multiple access, and cooperative communications.

JIANHUA GE received the Ph.D. degree from the School of Telecommunications Engineering, Xidian University, Xi'an, China, in 1990. He was involved in digital television (DTV) standardization as a DTV Technical Expert. He is currently a Professor and the Deputy Director of the State Key Laboratory of Integrated Services Networks, School of Telecommunications Engineering, Xidian University. His research interests include digital communications, digital video broadcasting, and performance enhancement techniques for 4G/B4G cellular communication systems.

QIFEI BU received the B.S. and M.S. degrees in telecommunications engineering from Xidian University, Xi'an, China, in 2012 and 2015, respectively, where he is currently pursuing the Ph.D. degree in communication and information system. He is very interested in wireless communication systems design and performance evaluation. His research interests include massive MIMO signal processing and performance analysis, physical layer security, non-orthogonal multiple access, and cooperative communications.

CHENSI ZHANG (M'16) received the B.S. and Ph.D. degrees in telecommunications engineering from Xidian University, Xi'an, China, in 2010 and 2015, respectively.

He is currently an Associate Professor with the State Key Laboratory of Integrated Services Networks, School of Telecommunications Engineering, Xidian University. His research interests include deep learning, cooperative communications, green communications, energy harvesting, and physical layer security. He is a member of the IEEE.